Systematic Use of Velocity and Acceleration Coefficients in the Kinematic Analysis of Single-DOF Planar Mechanisms

Raffaele Di Gregorio
Department of Engineering, University of Ferrara
Via Saragat,1; 44122 FERRARA; Italy
T: +39-0532-974828, F: +39-0532-974870
E: raffaele.digregorio@unife.it

Abstract
In single-degree-of-freedom (DOF) mechanisms, velocity coefficients (VCs) and their 1st derivative with respect to the generalized coordinate (acceleration coefficients (ACs)) only depend on the mechanism configuration. In addition, if the mechanism is a planar linkage (i.e., a mechanism containing only lower pairs), complex numbers are an easy-to-use tool for writing linkage's loop equations that are formally differentiable and are the only constraint equations of linkages. Actually, the use of complex numbers for systematically writing the constraint equations of planar mechanisms is often limited to linkages. The possible presence of higher pairs in these mechanisms is usually managed through either equivalent linkages or apparent velocity/acceleration equations. Both these methods are simple to implement for a single mechanism configuration, but become cumbersome when continuous motion has to be analyzed. Other approaches use ad hoc auxiliary equations. Here, first, a general notation that brings to select particular auxiliary equations is proposed; then, such notation is adopted to propose an algorithm that systematically uses VCs and ACs for solving the kinematic-analysis problems of single-DOF planar mechanisms. The proposed notation and algorithm, over being efficient enough for constituting the kinematic block of any dynamic model of these mechanisms, are easy to present planar kinematics, with the complex-number method extended to higher pairs, in graduate and/or undergraduate courses.

KEYWORDS: planar mechanism, velocity coefficient, acceleration coefficient, rolling contact, sliding contact, noncircular gears, higher education.

1. Introduction
Single-DOF planar linkages are present in many applications. Their technical relevance justifies the wide literature (see [1, 2], for Refs.) devoted to them.

Developing general-purpose software that solves their kinematic analysis (i.e., position, velocity and acceleration analyses) requires the adoption of a standardized procedure to reduce the analysis of a generic linkage to those of a small set of simpler problems easy to solve. Structural decomposition [3] based on Assur groups (AGs) [4, 5] is the most known of these procedures. Such procedure decomposes the linkage into "drivers" whose motion is known and AGs whose kinematics is analytically solvable starting from position, velocity and acceleration of the connecting points.

Other procedures [2] rely on systematic ways for writing the constraint equations of linkages. The vector-loop method is one of the possible ways for systematically writing linkages' constraint equations. Such method is diffusely adopted both to present mechanism kinematics in graduate and/or undergraduate courses (see [2], for instance) and to systematically solve position-analysis problems [6, 7]. The use of complex numbers[1] for representing planar vectors facilitates the implementation of this method.

Even though most mechanisms are linkages[2] (i.e., contain only lower pairs), relevant mechanism families (mechanisms with cams and/or gears) contain higher pairs. Thus, in graduate and/or undergraduate courses, presenting exhaustive analytical/numerical techniques for the kinematic analysis of (at least) planar mechanisms is a primary need.

Kinematic analysis of mechanisms may be implemented by writing the constraint equations together with their first and second time derivatives. The vector-loop method brings to write loop (closure) equations, which, for planar mechanisms, are easy to write in a systematic way by using the complex-number method. Unfortunately, such equations constitute the complete set of constraint equations only for linkages. Differently,

[1] The geometric interpretation of complex numbers [22, 23] is dated back to Wessel (1797), Argand (1806) and Gauss (1831). An exhaustive presentation of analytic plane geometry through complex numbers is reported in [23]; whereas planar kinematics through complex numbers is fully presented in [24] and, in a less extensive way, in [1, 25].
[2] The IFToMM terminology [8] is adopted in all the paper.

when higher pairs are present in a mechanism, the set of constraint equations must contain suitable additional equations that integrate the loop equations.

Planar mechanisms contain only four types of kinematic pairs: two lower-pair types (i.e., revolute (R) or prismatic (P) pairs) and two higher-pair types (i.e., rolling (R_c) or sliding (S_c) contacts). In these mechanisms, the possible presence of higher pairs is often managed through equivalent linkages [9, 24] or apparent velocity/acceleration equations [10], which are both simple to implement for a single mechanism configuration, but become cumbersome when continuous motion has to be analyzed. Other approaches use ad hoc auxiliary equations [1, 11].

In single-DOF mechanisms, the ratios between the secondary-variable[3] rates and the generalized-coordinate rate depend only on the mechanism configuration and are periodic functions when mapped as a function of the generalized coordinate [1]. Such ratios are named velocity coefficients (VCs) [1]. In the literature, VCs together with their 1st derivative with respect to the generalized coordinate (acceleration coefficients (ACs)) have been exploited to study both the kinematics (see [1, 12], for instance and Refs.) and the dynamics [13, 14] of single-DOF planar mechanisms.

This paper, firstly, extends the complex-number method to planar mechanisms with higher pairs by proposing a general notation that brings to select particular auxiliary equations; secondly, it presents a general algorithm for solving the kinematic analysis of single-DOF planar mechanisms. Such algorithm starts by writing the constraint equations with the proposed general notation; then, it computes one VC and one AC for each movable link by solving two linear systems, easy to deduce from the written constraint equations, and uses these VCs and ACs to calculate any velocity and/or acceleration of the mechanism. The proposed algorithm is globally novel. Also, it is efficient enough to be the kinematic block of any dynamic model of these mechanisms, and it lends itself to present planar kinematics in graduate and/or undergraduate courses.

The paper is organized as follows. Sections 2 and 3, over providing some background concepts, present the higher-pair modeling in the frame of the complex-number method, and the adopted general notation, respectively. Then, section 4 presents the algorithm; and, section 5 applies it to three case studies. Eventually, section 6 draws the conclusions.

2. Higher-Pair Modeling

Figure 1 shows a conjugate profile, fixed to the k-th link of a planar mechanism, that has to come into contact with another conjugate profile to form an higher pair of that mechanism. In Fig. 1, the reference Oxy is an

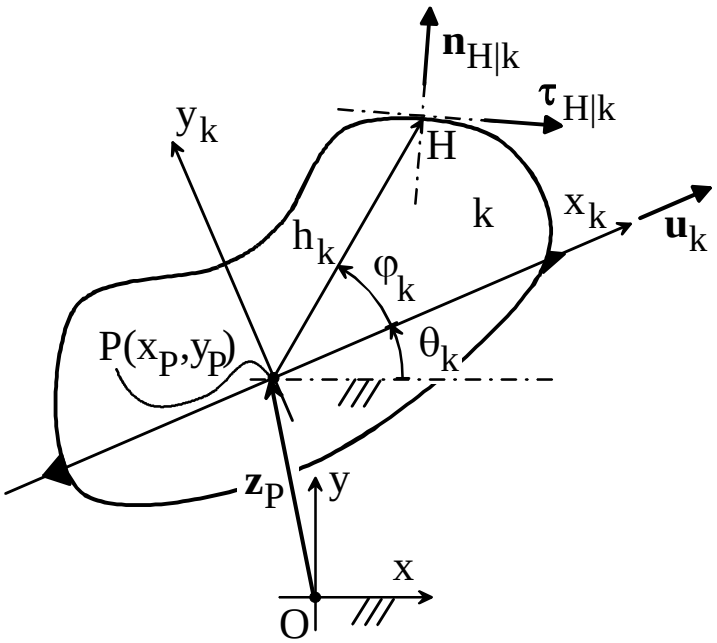

Figure 1: A conjugate profile fixed to the k-th link of a planar mechanism: notation.

[3] Hereafter, with reference to a single-DOF mechanism, the phrase "generalized coordinate" will denote the input variable of the kinematic analysis; whereas, the phrase "secondary variable" will denote a geometric parameter that changes its value during the motion of the linkage and is not the generalized coordinate.

Argand plane (A-plane) fixed to the mechanism frame; whereas, the reference Px_ky_k is an A-plane fixed to link k. h_k and φ_k are polar coordinates that locate a generic point, H, of the conjugate profile in the A-plane Px_ky_k through the complex number $\mathbf{h}_k=h_k\exp(\mathbf{i}\varphi_k)\equiv x_{H|k}+\mathbf{i}y_{H|k}$. In the A-plane Oxy, the position of link k is given by the complex number $\mathbf{z}_P=x_P+\mathbf{i}y_P$, where $\mathbf{i}$ is the imaginary unit $\sqrt{-1}$, that locates a generic point, P, fixed to link k; also, link-k's orientation is given by the unit complex number $\mathbf{u}_k=\exp(\mathbf{i}\theta_k)$.

For the sake of brevity, hereafter, the expression "complex number measured in the A-plane" will mean "complex number associated to the free planar vector measured in the Cartesian reference associated to that A-plane"[4]. With this terminology, the following statement holds "the product of $\mathbf{u}_k$ by a complex number measured in the A-plane Px_ky_k yields the complex number associated to the same free vector but measured in the A-plane Oxy". Thus, the complex number $\mathbf{z}_k=\mathbf{h}_k\mathbf{u}_k$ is associated to the free vector $(\mathbf{H}-\mathbf{P})$ (see Fig. 1) measured in Oxy, and the complex number $(\mathbf{z}_P+\mathbf{z}_k)$ locates point H in the A-plane Oxy. $\boldsymbol{\tau}_{H|k}$ is the unit complex number measured in Px_ky_k that is associated to the unit vector tangent to the conjugate profile at point H, and $\mathbf{n}_{H|k}=\mathbf{i}\,\boldsymbol{\tau}_{H|k}$. $\boldsymbol{\tau}_{H|k}$ and $\mathbf{n}_{H|k}$ define a local A-plane, fixed to link k, with point H as origin and axes that are tangent and normal at H to the conjugate profile.

The shape of a conjugate profile is usually given through parametric equations deduced to manufacture it with CNC machining tools [15, 16]. Hereafter, without losing generality, the analytic expression of the profile will be generically indicated through the two parametric equations $h_k=h_k(\psi_k)$ and $\varphi_k=\varphi_k(\psi_k)$, where ψ_k is the curve parameter. With this notation, $\boldsymbol{\tau}_{H|k}$ can be analytically expressed as follows (by definition, $x_{H|k}=h_k\cos\varphi_k$ and $y_{H|k}=h_k\sin\varphi_k$):

$$\tau_{H|k}=\frac{x'_{H|k}+\mathbf{i}\,y'_{H|k}}{\sqrt{(x'_{H|k})^2+(y'_{H|k})^2}} \tag{1a}$$

where

$$x'_{H|k}=\frac{dx_{H|k}}{d\psi_k},\qquad y'_{H|k}=\frac{dy_{H|k}}{d\psi_k}. \tag{1b}$$

Eventually, the infinitesimal arc length of the conjugate profile at H is

$$ds_k=\sqrt{(x'_{H|k})^2+(y'_{H|k})^2}\;d\psi_k \tag{2}$$

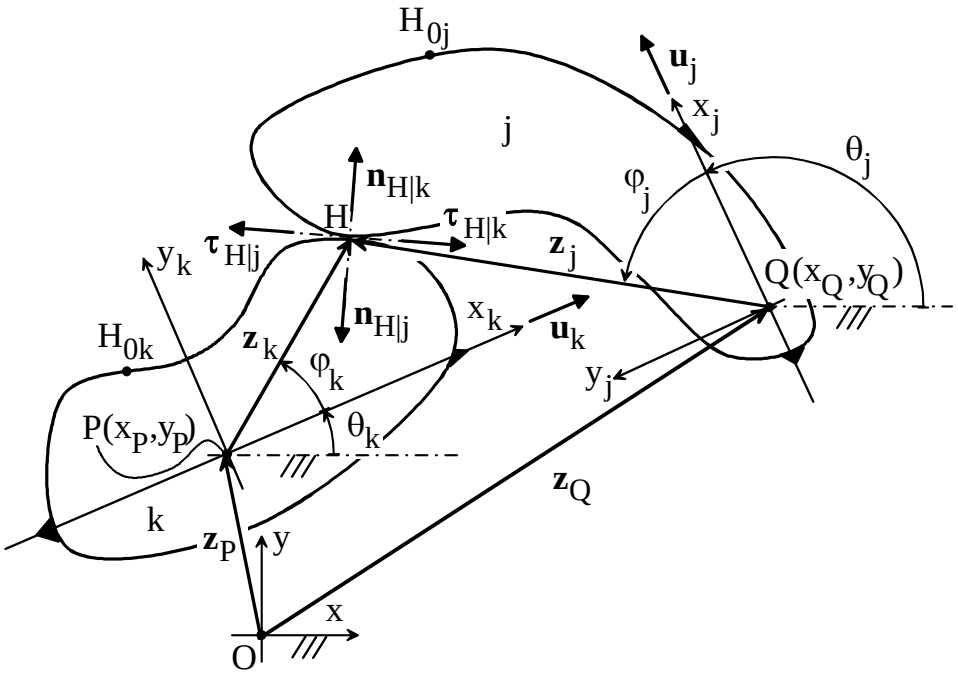

Figure 2: Two conjugate profiles in contact with each other at point H.

[4] Remind that the set of the free planar vectors measured in a given Cartesian reference is isomorphic to the complex numbers represented in the A-plane associated to that Cartesian reference.

2.1. Rolling Contact:

By using the notation of Fig. 1, Fig. 2 shows two links, k and j, that come into contact with one another at point H. If a rolling contact is present at point H, the two conjugate profiles that form the higher pair are indeed centrodes, and can be interpreted as the centrodes of two mating noncircular gears [17]. In this case, points H_{0k} and H_{0j} of Fig. 2 are the reference points of the two centrodes that come into contact with one another during the mechanism assembly; due to the rolling constraint, the lengths of the two arcs $\overset{\frown}{H_{0k}H}$ and $\overset{\frown}{H_{0j}H}$ are always equal.

With reference to Fig. 2, the closure equation of the loop passing through point H, in complex form, is

$$\mathbf{z}_P + \mathbf{z}_k = \mathbf{z}_Q + \mathbf{z}_j \tag{3}$$

where $\mathbf{z}_P = x_P + \mathbf{i}y_P$, $\mathbf{z}_Q = x_Q + \mathbf{i}y_Q$, $\mathbf{z}_k = \mathbf{h}_k\mathbf{u}_k$, and $\mathbf{z}_j = \mathbf{h}_j\mathbf{u}_j$ with $\mathbf{h}_k = h_k\exp(\mathbf{i}\varphi_k) \equiv x_{H|k} + \mathbf{i}y_{H|k}$, $\mathbf{h}_j = h_j\exp(\mathbf{i}\varphi_j) \equiv x_{H|j} + \mathbf{i}y_{H|j}$, $\mathbf{u}_k = \exp(\mathbf{i}\theta_k)$, and $\mathbf{u}_j = \exp(\mathbf{i}\theta_j)$.

Moreover, Eq. (1) holds for $\boldsymbol{\tau}_{H|k}$; whereas, for $\boldsymbol{\tau}_{H|j}$, the following expression holds

$$\tau_{H|j} = \frac{x'_{H|j} + \mathbf{i}\, y'_{H|j}}{\sqrt{(x'_{H|j})^2 + (y'_{H|j})^2}} \tag{4a}$$

with

$$x'_{H|j} = \frac{dx_{H|j}}{d\psi_j}, \quad y'_{H|k} = \frac{dy_{H|j}}{d\psi_j}, \tag{4b}$$

where ψ_j is the curve parameter of the two parametric equations $h_j = h_j(\psi_j)$ and $\varphi_j = \varphi_j(\psi_j)$, which define the shape of the centrode fixed to link j. Eventually, $ds_j = \sqrt{(x'_{H|j})^2 + (y'_{H|j})^2}\, d\psi_j$ is the infinitesimal arc length of the centrode, fixed to link j, at H, $\mathbf{n}_{H|k} = \mathbf{i}\,\boldsymbol{\tau}_{H|k}$ and $\mathbf{n}_{H|j} = \mathbf{i}\,\boldsymbol{\tau}_{H|j}$.

With these notations, the contact of the two centrodes at H can be imposed with the auxiliary (constraint) equation ($\underline{\mathbf{a}}$ denotes the complex conjugate of the complex number $\mathbf{a}$)

$$\mathrm{Re}(\mathbf{i}\,\boldsymbol{\tau}_{H|k}\,\mathbf{u}_k\,\underline{\boldsymbol{\tau}}_{H|j}\,\underline{\mathbf{u}}_j) = 0 \tag{5}$$

which simply imposes that, if $\mathbf{n}_{H|k}$ and $\boldsymbol{\tau}_{H|j}$ are both measured in the A-plane Oxy, they are associated to two mutually orthogonal free vectors[5] measured in Oxy.

Equation (5) can be expanded and simplified as follows:

$$\left(-y'_{H|k}x'_{H|j} + x'_{H|k}y'_{H|j}\right)\cos(\theta_k - \theta_j) - \left(x'_{H|k}x'_{H|j} + y'_{H|k}y'_{H|j}\right)\sin(\theta_k - \theta_j) = 0 \tag{6}$$

Equation (6) takes into account only the contact between the two profiles. Thus, another constraint equation has to be added which analytically expresses the rolling condition. Such equation has the differential form $ds_j = ds_k$, which can be integrated and expanded to give the following constraint equation

$$\int_{H_{0j}}^{H} \sqrt{(x'_{H|j})^2 + (y'_{H|j})^2}\, d\psi_j = \int_{H_{0k}}^{H} \sqrt{(x'_{H|k})^2 + (y'_{H|k})^2}\, d\psi_k \tag{7}$$

Equation (7) involves only the parametric curves of the two profiles and, due to the rolling nature of the contact, it can always state a one-to-one relationship between the two curve parameters ψ_j and ψ_k, that is, it can always be put in either of the two forms $\psi_j = \psi_j(\psi_k)$ or $\psi_k = \psi_k(\psi_j)$.

Equations (6) and (7) are the two auxiliary (constraint) equations that must be added to the loop equation (i.e., complex Eq. (3)) for modeling the rolling contact. Thus, in this case, the relative motion between links k and j is constrained by four scalar equations that contain five unknowns: $(x_P - x_Q)$, $(y_P - y_Q)$, $(\theta_k - \theta_j)$, ψ_j and ψ_k. This result is consistent with the fact that a rolling contact has one degree of freedom (DOF) and proves the correctness of the model.

Equations (6) and (7) can be combined into the unique complex equation

$$\mathbf{z}_{Rc}(\psi_k, \psi_j, \theta_k, \theta_j) = 0 \tag{8}$$

where the complex number $\mathbf{z}_{Rc} = x_{Rc} + \mathbf{i}\, y_{Rc}$ is defined by the relationships

[5] It is worth reminding that the real part of ($\mathbf{a}\,\underline{\mathbf{b}}$) is equal to the dot product of the two free vectors associated to the complex numbers $\mathbf{a}$ and $\mathbf{b}$, respectively.

$$x_{Rc} = \left[\left(- y'_{H|k} x'_{H|j} + x'_{H|k} y'_{H|j} \right) \cos(\theta_k - \theta_j) - \left(x'_{H|k} x'_{H|j} + y'_{H|k} y'_{H|j} \right) \sin(\theta_k - \theta_j) \right] \tag{9a}$$

$$y_{Rc} = \left[\int_{H_{0j}}^{H} \sqrt{(x'_{H|j})^2 + (y'_{H|j})^2}\ d\psi_j - \int_{H_{0k}}^{H} \sqrt{(x'_{H|k})^2 + (y'_{H|k})^2}\ d\psi_k \right] \tag{9b}$$

2.2. Sliding Contact:

With reference to Fig. 2, if a sliding contact occurs at point H, Eq. (6), which imposes the contact between the conjugate profiles, is still valid; whereas, the relationship between the arc lengths of the two profiles (i.e., Eq. (7)) is not valid any longer, that is, the two curve parameters ψ_j and ψ_k are independent from one another. As a consequence, in this case, the relative motion between links k and j is constrained by only three equations: the real and the imaginary parts of Eq. (3) (i.e., the loop equation), and Eq. (6). These three equations contain the same five unknowns as before (i.e., $(x_P - x_Q)$, $(y_P - y_Q)$, $(\theta_k - \theta_j)$, ψ_j and ψ_k), which is consistent with the fact that a sliding contact has two DOF.

Sliding-contact's auxiliary constraint equation (i.e., Eq. (6)) can be put in complex form as follows:

$$\mathbf{z}_{Sc}(\psi_k, \psi_j, \theta_k, \theta_j) = 0 \tag{10}$$

where the complex number $\mathbf{z}_{Sc} = x_{Sc} + \mathbf{i}\, y_{Sc}$ is defined by the relationships

$$x_{Sc} = \left[\left(- y'_{H|k} x'_{H|j} + x'_{H|k} y'_{H|j} \right) \cos(\theta_k - \theta_j) - \left(x'_{H|k} x'_{H|j} + y'_{H|k} y'_{H|j} \right) \sin(\theta_k - \theta_j) \right], \qquad y_{Sc} = 0. \tag{11}$$

3. General Notation

Planar mechanisms feature a number, m, of links connected by a number, c_1, of single-DOF kinematic pairs (i.e., whose type is R or P or R_c) and a number, c_2, of sliding contacts (S_c pairs), which are two-DOF kinematic pairs. According to Gruebler's formula [1], in single-DOF planar mechanisms m, c_1, and c_2 are related by the following relationship:

$$c_1 = 1.5\ m - 0.5\ c_2 - 2 \tag{12}$$

Their topology is representable through graphs (see [1] for details and further Refs.) whose nodes and edges refer to links and kinematic pairs, respectively. The loops appearing in these graphs geometrically individuate closed polygonal chains (circuits), embedded in the linkage. The vertices of these circuits are either points of R-pair axes, or contact points of higher pairs (i.e., R_c or S_c pairs), or points of P-pair sliding directions, which are fixed to one or the other of the two links joined by the P pair; whereas, their edges are either constant-length segments fixed to one link or variable-length segments corresponding to the joint variables of the P pairs or variable-lengths distances of higher-pairs' contact points from points fixed to either of the two links joined by those contacts. According to Euler formula [1], the number, a, of independent circuits of single-DOF planar mechanisms is

$$a = 0.5\ m + 0.5\ c_2 - 1 \tag{13}$$

Mechanisms' loop equations are deducible by analytically writing the vector equations that the independent circuits (ICs) represent from a geometric point of view. In single-DOF planar mechanisms, if the free vectors associated to the edges of the circuits are represented through complex numbers, the loop equations are obtained by equating to zero the algebraic sum of these complex numbers.

This approach can be implemented through the following steps:

i) the links are numbered from 1 to m and the number, a, of ICs is computed from Eq. (13);

ii) by inspecting all the kinematic pairs, c_1+c_2 points, A_t for $t = 1,\ldots, c_1+c_2$, (one for each pair), which are the contact points of the higher pairs plus points that belong either to an R-pair axis or to a line parallel to a P-pair sliding direction, are selected;

iii) among the points A_t for $t = 1,\ldots, c_1+c_2$, the couples of points that can be joined through an oriented segment either embedded in a link or belonging to a line parallel to a P-pair sliding direction are joined;

iv) the net of oriented segments deduced in step (iii) is analyzed and, through the graph of the linkage, the ICs are chosen; then, a complex number is associated to each oriented segment belonging to the chosen ICs, and the loop equations are written by assigning a conventional positive direction (clockwise or counterclockwise) to each IC.

The resulting system of loop equations has the following form

$$\sum_{k\in L_j} \pm \mathbf{z}_{kj} = 0 \qquad j = 1, \ldots, a \qquad (14)$$

where L_j is a set collecting the integer numbers that identify the links traversed by the j-th IC, $\mathbf{z}_{kj}$ is the complex number associated to the k-th edge of the j-th IC, and the sign + or – depends on whether the direction of the oriented segment represented by $\mathbf{z}_{kj}$ concurs or not with the positive direction (clockwise or counterclockwise) assigned to the j-th IC.

Figure 3 shows a generic k-th link traversed by q ICs, which contains the linear guide of a P-pair that connects it to a slider fixed in the s-th link, and the contact point, A_{p+i}, of an higher pair that connects it to the w-th link [h_{ki} (h_{wi}) and φ_{ki} (φ_{wi}) are the polar coordinates that define the conjugate profile fixed to the k-th link (to the w-th link) as a function of the curve parameter ψ_{ki} (the curve parameter ψ_{wi})]. With reference to Fig. 3, the possible $\mathbf{z}_{kj}$ that can be defined are

$$\mathbf{z}_{kj} = \mathbf{a}_{kj}\, \mathbf{u}_k \qquad j \in N_k = \{n_{k1}, \ldots, n_{kq}\} \subseteq \{1, \ldots, a\} \qquad (15a)$$
$$\mathbf{z}_{sj} = d_s\, \mathbf{u}_s \qquad (15b)$$

where, N_k is the subset of {1, …, a} that collects the integer numbers identifying the ICs passing through the k-th link. s is the number identifying the link that, in the j-th IC, follows[6] the k-th link. d_s is the variable length of the segment $A_{(p+r)}A_g$ (i.e., it is the joint variable of the P pair),

$$\mathbf{a}_{kj} = a_{kr} \exp(\mathbf{i}\alpha_{kr}) \qquad \mathbf{u}_k = \exp(\mathbf{i}\theta_k), \qquad \mathbf{u}_s = \exp(\mathbf{i}\alpha_s)\, \mathbf{u}_k, \qquad (16)$$

with $a_{kr}=h_{ki}(\psi_{ki})$ and $\alpha_{kr}= \varphi_{ki}(\psi_{ki})$ for $j=n_{ki}$ (i.e., for r=i); otherwise (i.e., $j\neq n_{ki}$ and $r\neq i$), with a_{kr} equal to the constant length of the segment $A_pA_{(p+r)}$ and α_{kr}, for $r \in \{2, \ldots, i-1, i+1, \ldots, q\}$, together with α_s, equal to constant angles. θ_k, for k = 1,…, m, is the angle that defines the orientation of the k-th link with respect to the frame.

The notation of Fig. 3 can always be applied to any link of a planar mechanism. This notation introduces one variable for each mobile link, which is an angle, θ_k, or a linear variable, d_s, if the link is connected to the previous one through an R-pair or a P-pair, respectively, and two curve parameters, ψ_{ki} and ψ_{wi}, for each R_c-pair or S_c-pair. Therefore, system (14) (i.e., the loop-equation system), which is a system of 2a [= $m+c_2-2$ (see Eq. (13))] scalar equations, contains $(m-1)+2(c_2+c_{Rc})$ variables where c_{Rc} is the number of R_c pairs.

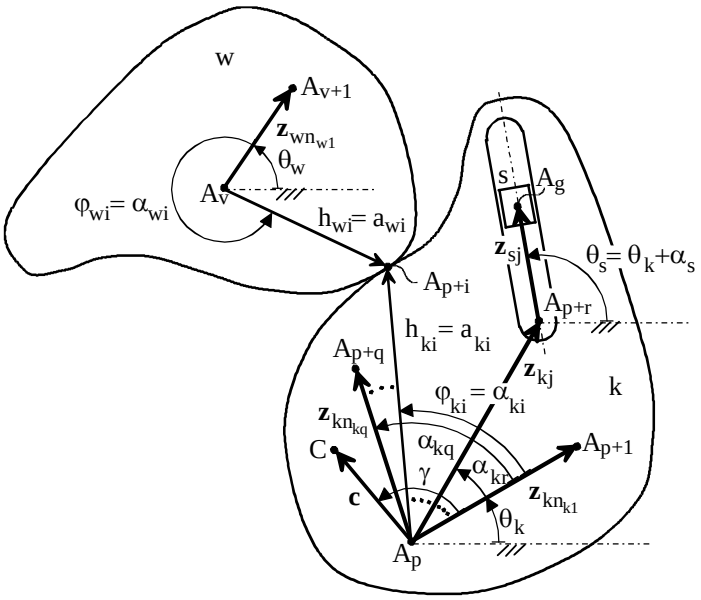

Figure 3: Notations: k-th link, traversed by q ICs, in contact with the w-th link at A_{p+i} through an higher pair, and containing the linear guide of a P-pair that connects it to a slider fixed in the s-th link.

[6] In the j-th IC the link order that states which is the previous or the next link is given by the positive direction (clockwise or counterclockwise) assigned to the j-th IC. Also, the order of the IC is given by the index j of system (3). Accordingly, the variables are defined.

The complete constraint-equation system is obtained by adding to system (14) one Eq. (8) for each R_c pair and one Eq. (10) for each S_c pair, that is, $(2c_{Rc}+c_2)$ more scalar equations. Such additional equations do not introduce further variables. As a consequence, the complete constraint-equation system consists of $m+2(c_{Rc}+c_2-1)$ scalar equations containing $(m-1)+2(c_2+c_{Rc})$ variables and can be solved once one of these variables (i.e., the chosen generalized coordinate) is assigned. Such system can be synthetically written as follows:

$$\sum_{k\in L_j} \pm \mathbf{z}_{kj} = 0 \qquad j = 1, \ldots, a \qquad (17a)$$

$$\mathbf{z}_{Rc|i}(\psi_{i1}, \psi_{i2}, \theta_{i1}, \theta_{i2}) = 0 \qquad i = 1, \ldots, c_{Rc} \qquad (17b)$$

$$\mathbf{z}_{Sc|n}(\psi_{n1}, \psi_{n2}, \theta_{n1}, \theta_{n2}) = 0 \qquad n = 1, \ldots, c_2 \qquad (17c)$$

with obvious meaning of the symbols[7].

With these notations, the 1st and 2nd time derivatives of the terms appearing in the constraint equations (17a), (17b), and (17c) are

$$\dot{\mathbf{z}}_{kj} = \dot{\varphi}\,(\mathbf{a}'_{kj}\varepsilon_{kr} + \mathbf{a}_{kj}\nu_k\mathbf{i})\mathbf{u}_k\,, \qquad \ddot{\mathbf{z}}_{kj} = \ddot{\varphi}\,(\mathbf{a}'_{kj}\varepsilon_{kr} + \mathbf{a}_{kj}\nu_k\mathbf{i})\mathbf{u}_k + \dot{\varphi}^2[\mathbf{a}'_{kj}\eta_{kr} + \mathbf{a}''_{kj}\varepsilon_{kr}^2 + 2\,\mathbf{a}'_{kj}\varepsilon_{kr}\nu_k\mathbf{i} + \mathbf{a}_{kj}(\lambda_k\mathbf{i} - \nu_k^2)]\mathbf{u}_k \qquad (18a)$$

$$\dot{\mathbf{z}}_{sj} = \dot{\varphi}\,(\delta_s + \mathrm{d}_s\nu_k\mathbf{i})\,\mathbf{u}_s\,, \qquad \ddot{\mathbf{z}}_{sj} = \ddot{\varphi}\,(\delta_s + \mathrm{d}_s\nu_k\mathbf{i})\mathbf{u}_s + \dot{\varphi}^2[\mu_s + 2\,\delta_s\nu_k\mathbf{i} + \mathrm{d}_s(\lambda_k\mathbf{i} - \nu_k^2)]\mathbf{u}_s \qquad (18b)$$

$$\dot{\mathbf{z}}_{Rc|i} = \dot{\varphi}\,\mathrm{L}_{Rc|i}\,, \qquad \ddot{\mathbf{z}}_{Rc|i} = \ddot{\varphi}\,\mathrm{L}_{Rc|i} + \dot{\varphi}^2\left(\mathrm{M}_{Rc|i} + \mathrm{G}_{Rc|i}\right) \qquad (18c)$$

$$\dot{\mathbf{z}}_{Sc|n} = \dot{\varphi}\,\mathrm{L}_{Sc|n}\,, \qquad \ddot{\mathbf{z}}_{Sc|n} = \ddot{\varphi}\,\mathrm{L}_{Sc|n} + \dot{\varphi}^2\left(\mathrm{M}_{Sc|n} + \mathrm{G}_{Sc|n}\right) \qquad (18d)$$

where[8]

$$\mathrm{L}_{Rc|i} = \frac{\partial\mathbf{z}_{Rc|i}}{\partial\psi_{i1}}\varepsilon_{i1} + \frac{\partial\mathbf{z}_{Rc|i}}{\partial\psi_{i2}}\varepsilon_{i2} + \frac{\partial\mathbf{z}_{Rc|i}}{\partial\theta_{i1}}\nu_{i1} + \frac{\partial\mathbf{z}_{Rc|i}}{\partial\theta_{i2}}\nu_{i2}\,, \qquad \mathrm{M}_{Rc|i} = \frac{\partial\mathbf{z}_{Rc|i}}{\partial\psi_{i1}}\eta_{i1} + \frac{\partial\mathbf{z}_{Rc|i}}{\partial\psi_{i2}}\eta_{i2} + \frac{\partial\mathbf{z}_{Rc|i}}{\partial\theta_{i1}}\lambda_{i1} + \frac{\partial\mathbf{z}_{Rc|i}}{\partial\theta_{i2}}\lambda_{i2} \qquad (19a)$$

$$\mathrm{L}_{Sc|n} = \frac{\partial\mathbf{z}_{Sc|n}}{\partial\psi_{n1}}\varepsilon_{n1} + \frac{\partial\mathbf{z}_{Sc|n}}{\partial\psi_{n2}}\varepsilon_{n2} + \frac{\partial\mathbf{z}_{Sc|n}}{\partial\theta_{n1}}\nu_{n1} + \frac{\partial\mathbf{z}_{Sc|n}}{\partial\theta_{n2}}\nu_{n2}\,, \qquad \mathrm{M}_{Sc|n} = \frac{\partial\mathbf{z}_{Sc|n}}{\partial\psi_{n1}}\eta_{n1} + \frac{\partial\mathbf{z}_{Sc|i}}{\partial\psi_{n2}}\eta_{n2} + \frac{\partial\mathbf{z}_{Sc|n}}{\partial\theta_{n1}}\lambda_{n1} + \frac{\partial\mathbf{z}_{Sc|i}}{\partial\theta_{n2}}\lambda_{n2} \qquad (19b)$$

$$\mathrm{G}_{Rc|i} = \frac{\partial\mathrm{L}_{Rc|i}}{\partial\psi_{i1}}\varepsilon_{i1} + \frac{\partial\mathrm{L}_{Rc|i}}{\partial\psi_{i2}}\varepsilon_{i2} + \frac{\partial\mathrm{L}_{Rc|i}}{\partial\theta_{i1}}\nu_{i1} + \frac{\partial\mathrm{L}_{Rc|i}}{\partial\theta_{i2}}\nu_{i2}\,, \qquad \mathrm{G}_{Sc|n} = \frac{\partial\mathrm{L}_{Sc|n}}{\partial\psi_{n1}}\varepsilon_{n1} + \frac{\partial\mathrm{L}_{Sc|n}}{\partial\psi_{n2}}\varepsilon_{n2} + \frac{\partial\mathrm{L}_{Sc|n}}{\partial\theta_{n1}}\nu_{n1} + \frac{\partial\mathrm{L}_{Sc|n}}{\partial\theta_{n2}}\nu_{n2} \qquad (19c)$$

In Eqs. (18) and (19), φ is the generalized coordinate. The following VCs and ACs have been introduced

$$\nu_k = \frac{\dot{\theta}_k}{\dot{\varphi}}\,, \qquad \delta_s = \frac{\dot{\mathrm{d}}_s}{\dot{\varphi}}\,, \qquad \varepsilon_{kr} = \frac{\dot{\psi}_{kr}}{\dot{\varphi}}\,, \qquad \lambda_k = \frac{\mathrm{d}\nu_k}{\mathrm{d}\varphi}\,, \qquad \mu_s = \frac{\mathrm{d}\delta_s}{\mathrm{d}\varphi}\,, \qquad \eta_{kr} = \frac{\mathrm{d}\varepsilon_{kr}}{\mathrm{d}\varphi}\,, \qquad (20)$$

together with the conjugate profile's geometric data $\mathbf{a}'_{kj}$ and $\mathbf{a}''_{kj}$ defined as follows

$$\mathbf{a}'_{kj} = \frac{\mathrm{d}\mathbf{a}_{kj}}{\mathrm{d}\psi_{kr}}\,, \qquad \mathbf{a}''_{kj} = \frac{\mathrm{d}^2\mathbf{a}_{kj}}{\mathrm{d}\psi_{kr}^2} = \frac{\mathrm{d}\mathbf{a}'_{kj}}{\mathrm{d}\psi_{kr}} \qquad (21)$$

where, if $\mathbf{z}_{kj}$ refers to a free vector pointing to an higher-pair contact point, ψ_{kr} is the curve parameter of the conjugate profile of that higher pair, which is fixed to the k-th link, and ε_{kr} (η_{kr}) is really a VC (an AC); otherwise, $\varepsilon_{kr} = \eta_{kr} = 0$, $\mathbf{a}'_{kj} = \mathbf{a}''_{kj} = 0$, and formulas (18a) are simplified as follows

$$\dot{\mathbf{z}}_{kj|0} = \dot{\varphi}\nu_k\mathbf{i}\mathbf{z}_{kj}\,; \qquad \ddot{\mathbf{z}}_{kj|0} = \ddot{\varphi}\nu_k\mathbf{i}\mathbf{z}_{kj} + \dot{\varphi}^2\,(\lambda_k\mathbf{i} - \nu_k^2)\mathbf{z}_{kj} \qquad (22)$$

---

[7] In Eqs. (17b) and (17c), the right subscripts i1 (n1) and i2 (n2), when they are subscript of ψ, stand for the kr index of the two curve parameters of the conjugate profiles in contact with each other in the higher pair the equation refers to; otherwise (i.e., when they are subscript of θ), they stand for the link numbers of the two links in contact with each other in the higher pair the equation refers to.

[8] Formulas (19c) are compact expressions where the partial derivatives of $\mathrm{L}_{Rc|i}$ ($\mathrm{L}_{Sc|i}$) must be done by considering the VCs as if they were independent variables.

It is worth noting that the VC and AC coefficients of formulas (19) are all known functions of the mechanism configuration, which can be analytically determined through the explicit expressions formulas (9) and (11) provide.

The kinematic interpretation of formulas (18a) and (18b) is (see Fig. 3)

$$\dot{\mathbf{z}}_{kj} - \dot{\varphi}\,\mathbf{a}'_{kj}\varepsilon_{kr}\,\mathbf{u}_k = \dot{\varphi}\,\nu_k\mathbf{i}\,\mathbf{z}_{kj} = \mathbf{v}_{A_{(p+r)}|k} - \mathbf{v}_{A_p|k}\,; \tag{23a}$$

$$\ddot{\mathbf{z}}_{kj} - \ddot{\varphi}\,\mathbf{a}'_{kj}\varepsilon_{kr}\,\mathbf{u}_k - \dot{\varphi}^2(\mathbf{a}'_{kj}\eta_{kr} + \mathbf{a}''_{kj}\varepsilon_{kr}^2 + 2\,\mathbf{a}'_{kj}\varepsilon_{kr}\nu_k\mathbf{i})\mathbf{u}_k = \ddot{\varphi}\nu_k\mathbf{i}\mathbf{z}_{kj} + \dot{\varphi}^2(\lambda_k\mathbf{i} - \nu_k^2)\mathbf{z}_{kj} = \mathbf{a}_{A_{(p+r)}|k} - \mathbf{a}_{A_p|k}\,; \tag{23b}$$

$$\dot{\mathbf{z}}_{sj} = \mathbf{v}_{Ag|s} - \mathbf{v}_{A_{(p+r)}|k}\,; \tag{23c}$$

$$\ddot{\mathbf{z}}_{sj} = \mathbf{a}_{Ag|s} - \mathbf{a}_{A_{(p+r)}|k}\,; \tag{23d}$$

where the symbol $\mathbf{v}_{B|f}$ ($\mathbf{a}_{B|f}$) denotes the velocity (acceleration), with respect to the frame, of a point B fixed to the f-th link, when expressed by using complex numbers. Moreover, with reference to the introduced notations and the loop n_{ki} of Fig. 3 (i.e., the path $A_pA_{(p+i)}A_v$), the following relationships hold (j= n_{ki}):

$$\dot{\mathbf{z}}_{kn_{ki}} - \dot{\mathbf{z}}_{wn_{ki}} = \mathbf{v}_{A_v|w} - \mathbf{v}_{A_p|k}\,; \tag{24a}$$

$$\ddot{\mathbf{z}}_{kn_{ki}} - \ddot{\mathbf{z}}_{wn_{ki}} = \mathbf{a}_{A_v|w} - \mathbf{a}_{A_p|k}\,; \tag{24b}$$

4. Kinematic Analysis through VCs and ACs

The first step of the kinematic analysis is the position analysis (PA). In single-DOF mechanisms, after the introduction of the above-defined notation, the PA consists in the determination of all the secondary variables, θ_k, ψ_{ki} and d_s, for an assigned value of the generalized coordinate, φ, by solving system (17). Such system can be always solved numerically (see [6, 7], for instance), and often it can also be solved analytically.

Once the PA has been solved all the complex numbers $\mathbf{z}_{kj}$ appearing in system (17) are known, and, together with $\dot{\varphi}$, become the input data of the velocity analysis (VA).

4.1. Velocity Analysis:

The 1st time derivative of the constraint Eqs. (17) provides the VA equations to solve. The VA equations can be automatically obtained by replacing, in system (17), each complex number with the expression of its 1st time derivative, formulas (18) provide. In so doing, the following system of VA equations is obtained

$$\dot{\varphi}\,D_j(\varphi) = 0 \qquad j = 1, \ldots, a \tag{25a}$$

$$\dot{\varphi}\,L_{Rc|i}(\varphi) = 0 \qquad i = 1, \ldots, c_{Rc} \tag{25b}$$

$$\dot{\varphi}\,L_{Sc|n}(\varphi) = 0 \qquad n = 1, \ldots, c_2 \tag{25c}$$

with $L_{Rc|i}$ ($L_{Sc|n}$) given by Eq. (19a) (Eq. (19b)), and

$$D_j(\varphi) = \sum_{k\in L_j} \pm[\mathbf{a}'_{kj}\varepsilon_{kr}\mathbf{u}_k + \nu_k\mathbf{i}\,(\mathbf{z}_{kj} + \beta_{kj}d_s\mathbf{u}_s) + \beta_{kj}\delta_s\mathbf{u}_s] \tag{26}$$

where β_{kj} is equal to 1 if, in the j-th IC, the k-th link is connected to the next through a P pair, otherwise it is equal to 0. Of course, the VC that corresponds to the variable chosen as generalized coordinate is equal to 1 and the VC that corresponds to the frame is equal to 0; as a consequence, the derivative with respect to φ of these two VCs are always equal to 0.

The coefficients D_j, $L_{Rc|i}$, and $L_{Sc|n}$ are linear combinations of the VCs whose coefficients are complex numbers that are all functions of φ and are known after the solution of the PA. System (25) is satisfied by imposing the vanishing of these coefficients, that is,

$$D_j = 0 \qquad j = 1, \ldots, a \tag{27a}$$

$$L_{Rc|i} = 0 \qquad i = 1, \ldots, c_{Rc} \tag{27b}$$

$$L_{Sc|n} = 0 \qquad n = 1, \ldots, c_2 \tag{27c}$$

System (27) is a linear system of $2(a+c_{Rc})+c_2$ [$= m + 2(c_{Rc}+c_2-1)$] scalar equations in $m+2(c_{Rc}+c_2-1)$ unknown VCs, which can be straightforwardly solved to obtain the values of the VCs. Once the VCs have been computed, the velocity of any point of the mechanism can be computed by exploiting formulas (18a), (18b), and their kinematic interpretation (23) and (24) as follows (see Fig. 3)

$$\mathbf{v}_{C|k} = \mathbf{v}_{A_p|k} + \mathbf{i}\,\dot{\varphi}\,\nu_k\,\mathbf{c} \tag{28}$$

where $\mathbf{v}_{A_p|k}$ is computed by using one of the paths that join point A_p to the frame through the edges of the ICs and formulas (18), (23) and (24) (i.e., it is a particular algebraic sum of the terms, given by formulas (18), associated to the edges of this path); whereas, $\mathbf{c} = c \exp(\mathbf{i}\gamma)\, \mathbf{u}_k$ with c equal to the constant length of the segment CA_p (see Fig.3).

Once the VA has been solved all the VCs appearing in Eq. (27) are known, and, together with the results of the PA, $\dot{\varphi}$, and $\ddot{\varphi}$ become the input data of the acceleration analysis (AA). Moreover, if either the analytic expression of the VCs have been determined or the VCs have been mapped as a function of the generalized coordinate, φ, the values of φ that make a VC null identify the linkage configurations where the secondary variable, the VC refers to, reaches an extreme value (i.e., the corresponding link is at a dead center position).

4.2. Acceleration Analysis:

The 2nd time derivative of the constraint Eqs. (17) provides the AA equations to solve. The AA equations can be automatically obtained by replacing, in system (17), each complex number with the expression of its 2nd time derivative, formulas (18) provide. In so doing, the following system of AA equations is obtained

$$\ddot{\varphi} D_j(\varphi) + \dot{\varphi}^2 [E_j(\varphi) - F_j(\varphi)] = 0 \qquad j = 1, \ldots, a \qquad (29a)$$

$$\ddot{\varphi}\, L_{Rc|i} + \dot{\varphi}^2 \left(M_{Rc|i} + G_{Rc|i} \right) = 0 \qquad i = 1, \ldots, c_{Rc} \qquad (29b)$$

$$\ddot{\varphi}\, L_{Sc|n} + \dot{\varphi}^2 \left(M_{Sc|n} + G_{Sc|n} \right) = 0 \qquad n = 1, \ldots, c_2 \qquad (29c)$$

with[9]

$$E_j(\varphi) = \sum_{k \in L_j} \pm [\mathbf{a}'_{kj} \eta_{kr} \mathbf{u}_k + \lambda_k \mathbf{i} (\mathbf{z}_{kj} + \beta_{kj} d_s \mathbf{u}_s) + \beta_{kj} \mu_s \mathbf{u}_s] \qquad (30a)$$

$$F_j(\varphi) = \sum_{k \in L_{jR}} \pm [\nu_k^2 \mathbf{z}_{kj} - (\mathbf{a}''_{kj} \varepsilon_{kr}^2 + 2 \mathbf{a}'_{kj} \varepsilon_{kr} \nu_k \mathbf{i}) \mathbf{u}_k - \beta_{kj} (2 \delta_s \nu_k \mathbf{i} - d_s \nu_k^2) \mathbf{u}_s] \qquad (30b)$$

Since D_j, $L_{Rc|i}$ and $L_{Sc|n}$ are all equal to zero (see system (27)), system (29) is satisfied by imposing that all the coefficients of $\dot{\varphi}^2$ vanish, that is

$$E_j = F_j \qquad j = 1, \ldots, a \qquad (31a)$$

$$M_{Rc|i} = -\, G_{Rc|i} \qquad i = 1, \ldots, c_{Rc} \qquad (31b)$$

$$M_{Sc|n} = -\, G_{Sc|n} \qquad n = 1, \ldots, c_2 \qquad (31c)$$

In system (31), F_j, $G_{Rc|i}$ and $G_{Sc|n}$ are all known since they contain only VCs and complex numbers, which are known after the PA solution; whereas, E_j, $M_{Rc|i}$ and $M_{Sc|n}$ are all linear combinations of the ACs whose coefficients are the same that multiply the corresponding VCs in the explicit expression of D_j, $L_{Rc|i}$ and $L_{Sc|n}$ (see Eqs. (19a), (19b) and (26)), respectively. Therefore, system (31) is a linear system of $2(a+c_{Rc})+c_2$ [$= m + 2(c_{Rc}+c_2-1)$] scalar equations in $m+2(c_{Rc}+c_2-1)$ unknown ACs, whose coefficient matrix of the unknowns is the same that appears in system (27) and its solution is straightforward, too.

Once the ACs have been computed by solving system (31), the acceleration of any point of the mechanism can be computed by exploiting formulas (18a), (18b), and their kinematic interpretation (23) and (24) as follows (see Fig. 3)

$$\mathbf{a}_{C|k} = \mathbf{a}_{A_p|k} + [\ddot{\varphi}\, \mathbf{i} \nu_k + \dot{\varphi}^2 (\mathbf{i} \lambda_k - \nu_k^2)] \mathbf{c} \qquad (32)$$

where $\mathbf{a}_{A_p|k}$ is computed by using one of the paths that join point A_p to the frame through the edges of the ICs and formulas (18), (23) and (24) (i.e., it is a particular algebraic sum of the terms, given by formulas (18), associated to the edges of this path).

5. Case Studies

In this section, the proposed kinematic-analysis algorithm is applied to three single-DOF mechanisms: the shaper mechanism shown in Fig. 4, the kinematic inversion of a geared five-bar mechanism shown in Fig. 5, and the circular cam with elliptic follower shown in Fig. 6.

---

[9] It is worth noting that $\frac{dD_j}{d\varphi} = E_j(\varphi) - F_j(\varphi)$, $\frac{dL_{Rc|i}}{d\varphi} = M_{Rc|i}(\varphi) + G_{Rc|i}(\varphi)$, and $\frac{dL_{Sc|n}}{d\varphi} = M_{Sc|n}(\varphi) + G_{Sc|n}(\varphi)$

5.1. Shaper Mechanism:

The shaper mechanism (Fig. 4) has m=6 and c_2=0; hence, Eqs. (12) and (13) yield c_1=7 and a=2. Accordingly, the inspection of the seven kinematic pairs brings to individuate the seven points A_r, r=1,…,7, shown in Fig. 4, as the vertices of the net containing all the circuits embedded in the mechanism. Inside this net, the two closed circuits $A_1A_3A_2A_1$ and $A_2A_7A_6A_5A_2$ are chosen as 1st and 2nd ICs, respectively.

5.1.1. Position Analysis

Since the shaper mechanism is a linkage its constraint equations coincide with its loop equations. The loop equations of the two above-mentioned ICs are

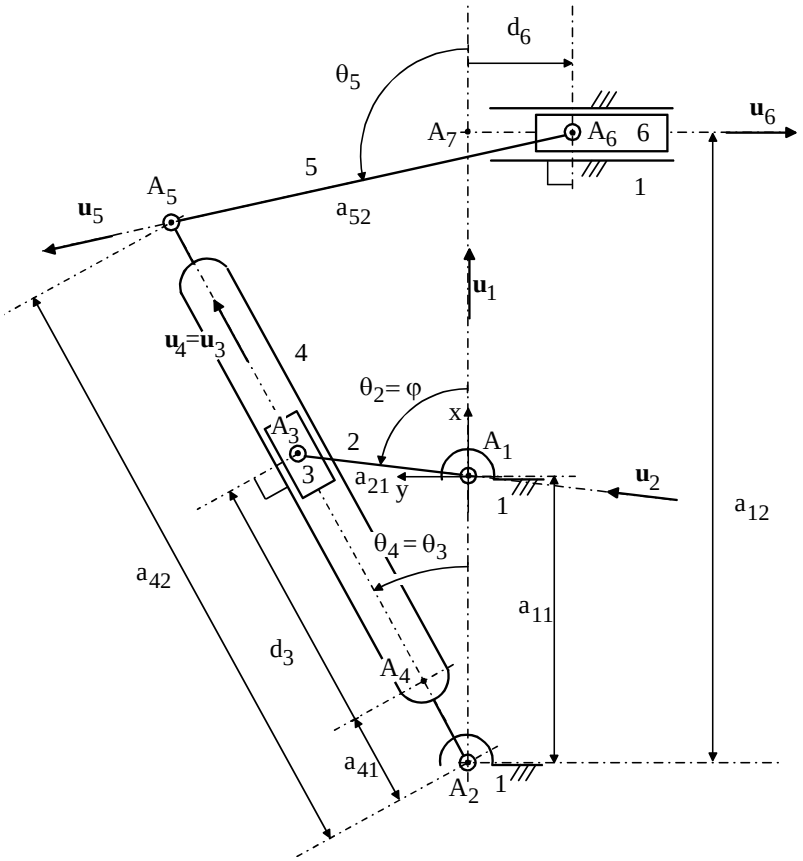

Figure 4: Shaper mechanism: kinematic scheme (link 1 is the frame) and notations (A_1xy is the reference of an Argand plane where **z**=x+**i**y).

$$\mathbf{z}_{11} + \mathbf{z}_{21} - \mathbf{z}_{41} - \mathbf{z}_{31} = \mathbf{0} \tag{33a}$$
$$\mathbf{z}_{12} + \mathbf{z}_{62} + \mathbf{z}_{52} - \mathbf{z}_{42} = \mathbf{0} \tag{33b}$$

where [$\mathbf{u}_2 = \exp(\mathbf{i}\varphi)$; $\mathbf{u}_3 = \mathbf{u}_4 = \exp(\mathbf{i}\theta_4)$; $\mathbf{u}_5 = \exp(\mathbf{i}\theta_5)$; $\mathbf{u}_6 = -\mathbf{i}$]

$$\mathbf{z}_{11} = a_{11};\quad \mathbf{z}_{21} = a_{21}\,\mathbf{u}_2;\quad \mathbf{z}_{41} = a_{41}\,\mathbf{u}_4;\quad \mathbf{z}_{31} = d_3\,\mathbf{u}_3; \tag{34a}$$
$$\mathbf{z}_{12} = a_{12};\quad \mathbf{z}_{62} = d_6\,\mathbf{u}_6;\quad \mathbf{z}_{52} = a_{52}\,\mathbf{u}_5;\quad \mathbf{z}_{42} = a_{42}\,\mathbf{u}_4; \tag{34b}$$

Once the generalized coordinate, φ, is assigned, system (33) becomes a non-linear system of four equations in the four secondary variables θ_4, θ_5, d_3 and d_6 which gives the following PA solutions in closed form ($\theta_4 \in [-90°, 90°]$; $\theta_5 \in [-180°, 180°]$)

$$\theta_4 = \arctan\left(\frac{a_{21}\sin\varphi}{a_{11}+a_{21}\cos\varphi}\right);\quad d_3 = \sqrt{(a_{21}\cos\varphi + a_{11})^2 + a_{21}^2\sin^2\varphi} - a_{41}; \tag{35a}$$

$$\theta_5 = \arccos\left(\frac{a_{42}\cos\theta_4 - a_{12}}{a_{52}}\right);\qquad d_6 = a_{52}\sin\theta_5 - a_{42}\sin\theta_4 \tag{35b}$$

Formulas (35) yield one value for θ_4 and d_3, and two values for θ_5 and d_6; thus, the PA of this linkage has two solutions.

5.1.2. Velocity Analysis

Equation (26) when applied to Eqs. (33a) and (33b) yields (ν_1=0; ν_2=1; λ_1=0; λ_2=0)

$$D_1(\varphi) = \mathbf{i}\,\mathbf{z}_{21} - \nu_4\,\mathbf{i}\,(\mathbf{z}_{41} + d_3\,\mathbf{u}_3) - \delta_3\,\mathbf{u}_3 \tag{36a}$$

$$D_2(\varphi) = \delta_6\,\mathbf{u}_6 + \nu_5\,\mathbf{i}\,\mathbf{z}_{52} - \nu_4\,\mathbf{i}\,\mathbf{z}_{42} \tag{36b}$$

where

$$\nu_4 = \frac{\dot\theta_4}{\dot\varphi}; \qquad \nu_5 = \frac{\dot\theta_5}{\dot\varphi}; \qquad \delta_3 = \frac{\dot d_3}{\dot\varphi}; \qquad \delta_6 = \frac{\dot d_6}{\dot\varphi}.$$

The linear system of two complex equations obtained by imposing that D_1 and D_2 are both equal to zero (see system (27a)) yields[10] the following VCs explicit expressions

$$\nu_4 = \frac{a_{21}\cos(\varphi-\theta_4)}{a_{41}+d_3}; \qquad \delta_3 = -a_{21}\sin(\varphi-\theta_4); \tag{37a}$$

$$\nu_5 = \frac{a_{21}a_{42}\cos(\varphi-\theta_4)\sin\theta_4}{(a_{41}+d_3)\,a_{52}\sin\theta_5}; \qquad \delta_6 = \frac{a_{21}a_{42}\cos(\varphi-\theta_4)\sin(\theta_4-\theta_5)}{(a_{41}+d_3)\sin\theta_5}; \tag{37b}$$

where θ_4, θ_5, and d_3 as functions of φ are given by Eqs. (35). The analysis of Eqs. (37a) and (37b) reveals that, when $\varphi-\theta_4=\pm 90°$ (i.e., when $\mathbf{u}_2$ is perpendicular to $\mathbf{u}_4$), links 4, 5 and 6 reach an extreme position. Link 5 reaches another extreme position also when θ_4=0; whereas link 3 reaches its extreme positions when $\varphi=\theta_4$, which can occur only when A_1, A_2, and A_3 (see Fig. 4) are aligned.

By using Eqs. (37), the velocity of any point can be computed as explained in subsection 4.1. For instance, Eq. (28) applied to the path $A_2A_5A_6$ (Fig. 4) yields the following expression of $\mathbf{v}_{A_6|6}$ (the last equality comes from the fact that D_2=0)

$$\mathbf{v}_{A_6|6} = \mathbf{v}_{A_5|5} - \mathbf{i}\,\dot\varphi\,\nu_5\,\mathbf{z}_{52} \equiv \mathbf{i}\,\dot\varphi\,(\nu_4\,\mathbf{z}_{42} - \nu_5\,\mathbf{z}_{52}) \equiv \dot\varphi\,\delta_6\,\mathbf{u}_6$$

5.1.3. Acceleration Analysis

Equations (30a) and (30b) when applied to Eqs. (33a) and (33b) yield (ν_1=0; ν_2=1; λ_1=0; λ_2=0)

$$E_1(\varphi) = -\lambda_4\,\mathbf{i}\,(\mathbf{z}_{41} + d_3\,\mathbf{u}_3) - \mu_3\,\mathbf{u}_3 \tag{38a}$$

$$F_1(\varphi) = \mathbf{z}_{21} - \nu_4^2\,\mathbf{z}_{41} + (2\,\delta_3\,\nu_4\,\mathbf{i} - d_3\,\nu_4^2)\,\mathbf{u}_3 \tag{38b}$$

$$E_2(\varphi) = \mu_6\,\mathbf{u}_6 + \lambda_5\,\mathbf{i}\,\mathbf{z}_{52} - \lambda_4\,\mathbf{i}\,\mathbf{z}_{42} \tag{38c}$$

$$F_2(\varphi) = \nu_5^2\,\mathbf{z}_{52} - \nu_4^2\,\mathbf{z}_{42} \tag{38d}$$

where F_1 and F_2 are two known complex expressions, and

$$\lambda_4 = \frac{d\nu_4}{d\varphi}; \quad \lambda_5 = \frac{d\nu_5}{d\varphi}; \quad \mu_3 = \frac{d\delta_3}{d\varphi}; \quad \mu_6 = \frac{d\delta_6}{d\varphi}.$$

The linear system of two complex equations obtained by imposing (see system (31a)) that E_1 and E_2 are equal to F_1 and F_2, respectively, yields the following ACs expressions

$$\lambda_4 = -\frac{2\delta_3\nu_4 + a_{21}\sin(\varphi-\theta_4)}{a_{41}+d_3}; \qquad \mu_3 = \nu_4^2(a_{41}+d_3) - a_{21}\cos(\varphi-\theta_4); \tag{39a}$$

$$\lambda_5 = \frac{a_{42}\{\nu_4^2(a_{41}+d_3)\cos\theta_4 - [2\delta_3\nu_4 + a_{21}\sin(\varphi-\theta_4)]\sin\theta_4\} - \nu_5^2 a_{52}(a_{41}+d_3)\cos\theta_5}{a_{52}(a_{41}+d_3)\sin\theta_5}; \tag{39b}$$

$$\mu_6 = \frac{a_{42}a_{52}\{\nu_4^2(a_{41}+d_3)\cos(\theta_4-\theta_5) - [2\delta_3\nu_4 + a_{21}\sin(\varphi-\theta_4)]\sin(\theta_4-\theta_5)\} - \nu_5^2 a_{52}^2(a_{41}+d_3)}{a_{52}(a_{41}+d_3)\sin\theta_5} \tag{39c}$$

[10] It is worth reminding that the solution formulas of the complex equation $x\mathbf{a}+y\mathbf{b}=\mathbf{c}$, with x and y real unknowns and **a**, **b** and **c** known complex coefficients, are ($\underline{\mathbf{z}}$ is the conjugate of **z**)

$$x = \frac{\mathrm{Im}(\mathbf{c}\underline{\mathbf{b}})}{\mathrm{Im}(\mathbf{a}\underline{\mathbf{b}})}, \qquad y = \frac{\mathrm{Im}(\mathbf{c}\underline{\mathbf{a}})}{\mathrm{Im}(\mathbf{b}\underline{\mathbf{a}})}.$$

where θ_4, θ_5, and d_3 as functions of φ are given by Eqs. (35); whereas, ν_4, ν_5, and δ_3 as functions of φ are given by Eqs. (37). The acceleration of any point can be computed by using Eqs. (39) (see subsection 4.2). For instance, Eq. (32) applied to the path $A_2A_5A_6$ (Fig. 4) yields $\mathbf{a}_{A_6|6} = \mathbf{a}_{A_5|5} - [\ddot{\varphi}\,\mathbf{i}\,\nu_5 + \dot{\varphi}^2(\mathbf{i}\lambda_5 - \nu_5^2)]\mathbf{z}_{52}$, whose expansion gives (the last equality comes from the fact that D_2=0 and E_2=F_2)

$$\mathbf{a}_{A_6|6} = \mathbf{i}\,\ddot{\varphi}\,(\nu_4\,\mathbf{z}_{42} - \nu_5\,\mathbf{z}_{52}) + \dot{\varphi}^2[(\mathbf{i}\lambda_4 - \nu_4^2)\mathbf{z}_{42} - (\mathbf{i}\lambda_5 - \nu_5^2)\mathbf{z}_{52}] \equiv (\ddot{\varphi}\,\delta_6 + \dot{\varphi}^2\mu_6)\,\mathbf{u}_6$$

5.2. A Kinematic Inversion of the Geared 5-bar Mechanism:

Figure 5 shows the kinematic scheme of a single-DOF planar mechanism with four links. Link 1 is the frame, link 2 and 3 are two mating gears, which are represented in Fig. 5 through their pitch circles, and link 4 is a rocker. Gears 2 and 3 are eccentrically hinged to the frame (link 1) and the rocker (link 4), respectively, while their pitch circles are in contact with each other at H through a rolling contact. A planet carrier (link 5) hinged at the geometric centers, points P and Q, of the two gears is present, too, but it is not shown in Fig. 5 since it simply keeps the mating of the two gears without affecting the mechanism motion. The mechanism of Fig. 5 is a kinematic inversion of the geared five-bar mechanism, which is a mechanism widely studied for many applications (see, for instance, [18 – 21]). It is worth noting that the equivalent-linkage method [9] fails in the analysis of this mechanism since, in this case, it gives an equivalent linkage with 2 DOF[11] (i.e., with one extra DOF).

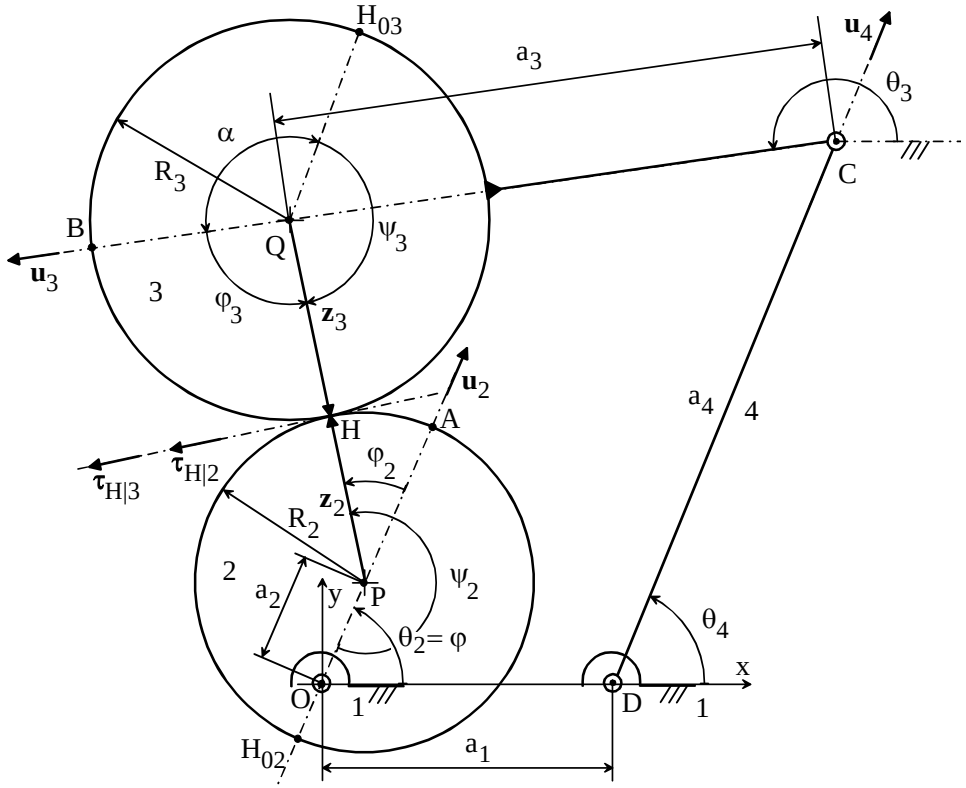

Figure 5: Kinematic scheme of a kinematic inversion of the geared five-bar mechanism [a rolling contact occurs at point H; the planet carrier (link 5) hinged at P and Q to the gears 2 and 3, respectively, is not shown since it does not affect the mechanism motion].

5.2.1. Position Analysis

With reference to Fig. 5, R_2 and R_3 are the radii of the pitch circles of gears 2 and 3, respectively; whereas, a_1, a_2, a_3, and a_4 are the lengths of the segments OD, OP, CQ, and CD, respectively. H_{02} and H_{03} are the two points that come into contact with each other at the mechanism assembly. The angles ψ_2 and ψ_3 are the adopted curve

[11] In general, the equivalent-linkage method always fails in eliminating a rolling contact when both the shapes of the conjugate profiles affect the relative motion between the links that come into contact with each other through the rolling contact. Indeed, in these cases, it always yield a linkage with one extra DOF with respect to the original mechanism.

parameters. Therefore, the parametric equations of the conjugate profiles and the analytic expressions of the unit complex number $\boldsymbol{\tau}_{H|2}$ and $\boldsymbol{\tau}_{H|3}$ are as follows:

- gear 2: $h_2=R_2$ and $\varphi_2=\psi_2-\psi_{02}$ with $\psi_{02}=\pi$, which yield $\mathbf{h}_2=h_2\exp(\mathbf{i}\varphi_2)\equiv x_{H|2}+\mathbf{i}y_{H|2}$, that is, $x_{H|2}=R_2\cos(\psi_2-\psi_{02})$, $y_{H|2}=R_2\sin(\psi_2-\psi_{02})$, and $\boldsymbol{\tau}_{H|2} = \mathbf{i}\exp[\mathbf{i}(\psi_2-\psi_{02})]$;

- gear 3: $h_3=R_3$ and $\varphi_3=\psi_{03}-\psi_3$ with $\psi_{03}=2\pi-\alpha$, which yield $\mathbf{h}_3=h_3\exp(\mathbf{i}\varphi_3)\equiv x_{H|3}+\mathbf{i}y_{H|3}$, that is, $x_{H|3}=R_3\cos(\psi_{03}-\psi_3)$, $y_{H|3}=R_3\sin(\psi_{03}-\psi_3)$, and $\boldsymbol{\tau}_{H|3}= -\mathbf{i}\exp[\mathbf{i}(\psi_{03}-\psi_3)]$.

With the adopted notations, the following relationships hold:

$$\mathbf{z}_2 = R_2\exp[\mathbf{i}(\psi_2-\psi_{02})]\,\mathbf{u}_2, \quad \mathbf{z}_3 = R_3\exp[\mathbf{i}(\psi_{03}-\psi_3)]\,\mathbf{u}_3, \tag{40a}$$

$$\mathbf{z}_P = a_2\,\mathbf{u}_2, \quad \mathbf{z}_Q = a_1 + a_4\,\mathbf{u}_4 + a_3\,\mathbf{u}_3 \tag{40b}$$

where $\mathbf{u}_k=\exp(\mathbf{i}\theta_k)$ for k=2,3,4.

The introduction of expressions (40a) and (40b) into Eq. (3) yields, for the mechanism of Fig. 5, the following loop equation:

$$a_2\,\mathbf{u}_2 + R_2\exp[\mathbf{i}(\psi_2-\psi_{02})]\,\mathbf{u}_2 = a_1 + a_4\,\mathbf{u}_4 + a_3\,\mathbf{u}_3 + R_3\exp[\mathbf{i}(\psi_{03}-\psi_3)]\,\mathbf{u}_3 \tag{41}$$

Moreover, the introduction of the above-reported expressions for $\mathbf{h}_2$ and $\mathbf{h}_3$ into Eqs. (6) and (7) gives the two auxiliary constraint equations

$$\begin{aligned}&[-\cos(\psi_2-\psi_{02})\sin(\psi_{03}-\psi_3) + \sin(\psi_2-\psi_{02})\cos(\psi_{03}-\psi_3)]\cos(\theta_2-\theta_3) + \\ &+ [\sin(\psi_2-\psi_{02})\sin(\psi_{03}-\psi_3) + \cos(\psi_2-\psi_{02})\cos(\psi_{03}-\psi_3)]\sin(\theta_2-\theta_3) = 0\end{aligned} \tag{42}$$

$$R_2\,\psi_2 = R_3\,\psi_3 \tag{43}$$

Equations (41), (42) and (43) constitute the complete set of constraint equations of this mechanism. They form a system of four scalar equations in five unknowns: θ_2, θ_3, θ_4, ψ_2, and ψ_3. θ_2 is chosen as generalized coordinate φ of the mechanism; the remaining 4 variables are all secondary variable whose expression as a function of φ can be computed by solving the constraint equation system.

Applying the trigonometric identities $\cos(x_1-x_2)=\cos(x_1)\cos(x_2)+\sin(x_1)\sin(x_2)$, and $\sin(x_1-x_2)=\sin(x_1)\cos(x_2)-\cos(x_1)\sin(x_2)$ to the two expressions in square brackets of Eq. (42) and, then, the trigonometric identity $\sin(x_1+x_2)=\sin(x_1)\cos(x_2)+\cos(x_1)\sin(x_2)$ to the resulting left-hand side of Eq. (42) transforms Eq. (42) as follows:

$$\sin(\psi_2+\psi_3+\theta_2-\theta_3-\psi_{02}-\psi_{03}) = 0 \tag{44}$$

The notations of Fig. 5 make it possible to select the following solution of Eq. (44) (i.e., of Eq.(42))

$$\psi_2+\psi_3+\theta_2-\theta_3-\psi_{02}-\psi_{03} = -\pi \tag{45}$$

Equation (45) replaces Eq. (42) into the constraint-equation system.

Equations (43) and (45) are two linear equations that, when solved with respect to ψ_2 and ψ_3, give the following explicit expressions

$$\psi_3 = r\,\psi_2 = p\,(\theta_3-\theta_2+\gamma) \tag{46a}$$

$$\psi_2 = (1-p)\,(\theta_3-\theta_2+\gamma) \tag{46b}$$

where the geometric constants $r=R_2/R_3$, $p= r/(1+r)$, and $\gamma=\psi_{02}+\psi_{03}-\pi = 2\pi-\alpha$ have been introduced.

The introduction of expressions (46a) and (46b) into Eq. (41), after some algebraic manipulation, yields

$$a_4\exp(\mathbf{i}\theta_4) = a_2\exp(\mathbf{i}\theta_2) + (\mathbf{b}_2-\mathbf{b}_3)\exp(\mathbf{i}\,p\theta_2)\exp[\mathbf{i}(1-p)\theta_3] - a_1 - a_3\exp(\mathbf{i}\theta_3) \tag{47}$$

where the complex constants

$$\mathbf{b}_2= R_2\exp\{\mathbf{i}[(1-p)\gamma-\psi_{02}]\} = -R_2\exp\{\mathbf{i}[(1-p)\psi_{03}]\}$$

$$\mathbf{b}_3= R_3\exp[\mathbf{i}(\psi_{03}-p\,\gamma)] = R_3\exp[\mathbf{i}(1-p)\psi_{03}]$$

have been introduced.

By equating the square of the absolute value of the left-hand side of Eq. (47) to the square of the absolute value of the right-hand side of the same equation, the variable θ_4 can be eliminated. So doing, the following scalar equation is obtained

$$\begin{aligned} a_4^2 = {} & a_2^2+(R_2+R_3)^2 + a_1^2+a_3^2- 2a_1\, a_2 \cos(\theta_2) + 2a_1\, a_3 \cos(\theta_3) - 2a_2\, a_3 \cos(\theta_3-\theta_2)+ \\ & - 2a_2\,(R_2+R_3)\cos[(1-p)\,(\theta_3-\theta_2+\psi_{03})] + 2(R_2+R_3)\, a_3 \cos[p(\theta_3-\theta_2+\psi_{03}) - \psi_{03}]+ \\ & +2a_1\,(R_2+R_3)\cos\mathbf{[}(1-p)(\theta_3+\psi_{03})+ p\theta_2] \end{aligned} \tag{48}$$

Equation (48), over the generalized coordinate θ_2, contains only θ_3. As a consequence, it can be numerically solved for each value of θ_2 (belonging to a discrete set of values of $[0, 2\pi]$), in order to find the corresponding value(s) of θ_3 that solve the constraint-equation system. Once θ_3 as a function of θ_2 has been computed, the values of ψ_2, and ψ_3 corresponding to each computed value of the two-tuple (θ_2, θ_3) can be immediately computed through Eqs. (46a) and (46b); whereas, the value of θ_4 corresponding to each computed value of the two-tuple (θ_2, θ_3) can be computed through Eq. (47) as ATAN2(Im(**z**(θ_2, θ_3)),Re(**z**(θ_2, θ_3))) where **z**(θ_2, θ_3) is the right-hand side of Eq. (47).

5.2.2. Velocity Analysis

The 1st time derivative of the simplified constraint-equation system constituted by Eqs. (43), (45), and (47) yields

$$\dot{\theta}_2\, D(\theta_2) = 0 \tag{49a}$$

$$\dot{\theta}_2\, L_{Rc}(\theta_2) = 0 \tag{49b}$$

where

$$D(\theta_2) = \{a_3\, \mathbf{i}\, \mathbf{u}_3 - \mathbf{i}(1-p)(\mathbf{b}_2-\mathbf{b}_3)\exp(\mathbf{i}\, p\theta_2)\exp[\mathbf{i}(1-p)\theta_3]\}\, \nu_3 + (a_4\, \mathbf{i}\, \mathbf{u}_4)\, \nu_4 - \mathbf{d} \tag{50a}$$

$$L_{Rc}(\theta_2) = (\varepsilon_2 + \varepsilon_3 + 1 - \nu_3) + \mathbf{i}\,(r\,\varepsilon_2 - \varepsilon_3) \tag{50b}$$

with $\mathbf{d} = a_2\, \mathbf{i}\, \mathbf{u}_2 + \mathbf{i}\, p\, (\mathbf{b}_2-\mathbf{b}_3)\exp(\mathbf{i}\, p\theta_2)\exp[\mathbf{i}(1-p)\theta_3]$, and

$$\nu_3 = \frac{\dot{\theta}_3}{\dot{\theta}_2}; \qquad \nu_4 = \frac{\dot{\theta}_4}{\dot{\theta}_2}; \qquad \varepsilon_2 = \frac{\dot{\psi}_2}{\dot{\theta}_2}; \qquad \varepsilon_3 = \frac{\dot{\psi}_3}{\dot{\theta}_2}.$$

Therefore, the VA equations obtained by equating to zero $D(\theta_2)$ and $L_{Rc}(\theta_2)$ (see Eqs.(27a) and (27b)) are

$$\{a_3\, \mathbf{i}\, \mathbf{u}_3 - \mathbf{i}(1-p)(\mathbf{b}_2-\mathbf{b}_3)\exp(\mathbf{i}\, p\theta_2)\exp[\mathbf{i}(1-p)\theta_3]\}\, \nu_3 + (a_4\, \mathbf{i}\, \mathbf{u}_4)\, \nu_4 = \mathbf{d} \tag{51a}$$

$$\varepsilon_2 + \varepsilon_3 - \nu_3 = -1 \tag{51b}$$

$$r\,\varepsilon_2 - \varepsilon_3 = 0 \tag{51c}$$

where **d** is a known complex number after the solution of the PA.

The solution of system (51) is:

$$\nu_3 = \frac{a_2\sin(\theta_2-\theta_4) - p\left(R_2+R_3\right)\sin[p\theta_2+\left(1-p\right)(\theta_3+\psi_{03})-\theta_4]}{a_3\sin(\theta_3-\theta_4) + \left(1-p\right)\left(R_2+R_3\right)\sin[p\theta_2+\left(1-p\right)(\theta_3+\psi_{03})-\theta_4]}, \tag{52a}$$

$$\nu_4 = \frac{a_2 a_3\sin(\theta_2-\theta_3) - a_2\left(1-p\right)\left(R_2+R_3\right)\sin[\left(1-p\right)(\theta_3-\theta_2+\psi_{03})] - a_3 p\,\left(R_2+R_3\right)\sin[p(\theta_2-\theta_3)+\left(1-p\right)\psi_{03}]}{-a_4\{a_3\sin(\theta_3-\theta_4) + \left(1-p\right)\left(R_2+R_3\right)\sin[p\theta_2+\left(1-p\right)(\theta_3+\psi_{03})-\theta_4]\}}, \tag{52b}$$

$$\varepsilon_2 = (1-p)\,(\nu_3 - 1), \qquad \varepsilon_3 = p\,(\nu_3 - 1). \tag{52c}$$

5.2.3. Acceleration Analysis

The time derivative of system (49) provides the following equations (see Eqs. (29a) and (29b))

$$\ddot{\theta}_2\, D(\theta_2) + \dot{\theta}_2^2[E(\theta_2) - F(\theta_2)] = 0 \tag{53a}$$

$$\ddot{\theta}_2\, L_{Rc}(\theta_2) + \dot{\theta}_2^2[M_{Rc}(\theta_2) + G_{Rc}(\theta_2)] = 0 \tag{53b}$$

where

$$E(\theta_2) = \{a_3\, \mathbf{i}\, \mathbf{u}_3 - \mathbf{i}(1-p)(\mathbf{b}_2-\mathbf{b}_3)\exp(\mathbf{i}\, p\theta_2)\exp[\mathbf{i}(1-p)\theta_3]\}\, \lambda_3 + (a_4\, \mathbf{i}\, \mathbf{u}_4)\, \lambda_4 \tag{54a}$$

$$F(\theta_2) = -a_2\, \mathbf{u}_2 + a_3\, \mathbf{u}_3\, \nu_3^2 + a_4\, \mathbf{u}_4\, \nu_4^2 + (R_2+R_3)\,[(1-p)\,\nu_3 + p]^2 \exp\{\mathbf{i}[p\theta_2 + (1-p)(\theta_3 + \psi_{03})] \tag{54b}$$

$$M_{Rc}(\theta_2) = (\eta_2 + \eta_3 - \lambda_3) + \mathbf{i}\,(r\,\eta_2 - \eta_3), \qquad G_{Rc}(\theta_2) = 0 \tag{54c}$$

with

$$\lambda_3 = \frac{dv_3}{d\theta_2}; \qquad \lambda_4 = \frac{dv_4}{d\theta_2}; \qquad \eta_2 = \frac{d\varepsilon_2}{d\theta_2}; \qquad \eta_3 = \frac{d\varepsilon_3}{d\theta_2}.$$

Therefore, in this case, the AA equations (see Eqs.(31a) and (31b)) are

$$\{a_3\,\mathbf{i}\,\mathbf{u}_3 - \mathbf{i}(1-p)(\mathbf{b}_2-\mathbf{b}_3)\exp(\mathbf{i}\,p\theta_2)\exp[\mathbf{i}(1-p)\theta_3]\}\,\lambda_3 + (a_4\,\mathbf{i}\,\mathbf{u}_4)\,\lambda_4 = F(\theta_2) \tag{55a}$$

$$\eta_2 + \eta_3 - \lambda_3 = 0 \tag{55b}$$

$$r\,\eta_2 - \eta_3 = 0 \tag{55c}$$

where $F(\theta_2)$ (see Eq. (54b)) is a known complex number after the solution of the PA and of the VA.

The solution of system (55) is:

$$\lambda_3 = \frac{a_2\cos(\theta_2-\theta_4) - v_3^2 a_3\cos(\theta_3-\theta_4) - a_4 v_4^2 - (R_2+R_3)[(1-p)v_3+p]^2\cos[p\theta_2+(1-p)(\theta_3+\psi_{03})-\theta_4]}{a_3\sin(\theta_3-\theta_4) + (1-p)(R_2+R_3)\sin[p\theta_2+(1-p)(\theta_3+\psi_{03})-\theta_4]}, \tag{56a}$$

$$\lambda_4 = \frac{g_4}{-a_4\{a_3\sin(\theta_3-\theta_4) + (1-p)(R_2+R_3)\sin[p\theta_2+(1-p)(\theta_3+\psi_{03})-\theta_4]\}}, \tag{56b}$$

$$\eta_2 = (1-p)\,\lambda_3, \qquad \eta_3 = p\,\lambda_3 \tag{56c}$$

where

$$g_4 = a_2a_3\cos(\theta_2-\theta_3) - a_3^2\,v_3^2 - a_4a_3v_4^2\cos(\theta_4-\theta_3) - a_3(R_2+R_3)[(1-p)\,v_3+p]^2\cos[p(\theta_2-\theta_3)+(1-p)\,\psi_{03}] +$$
$$-(R_2+R_3)[(1-p)v_3+p]^2(1-p)(R_2+R_3) + a_2(1-p)(R_2+R_3)\cos[(1-p)(\theta_2+\theta_3+\psi_{03})] +$$
$$-a_3v_3^2(1-p)(R_2+R_3)\cos[p(\theta_2-\theta_3)+(1-p)\,\psi_{03}] - a_4v_4^2\,(1-p)(R_2+R_3)\cos[p\theta_2+(1-p)(\theta_3+\psi_{03})-\theta_4].$$

5.3. Circular Cam with Elliptic Follower:

Figure 6 shows the kinematic scheme of a single-DOF planar mechanism with three links. Link 1 is the frame, link 2 is a circular cam eccentrically hinged to the frame, and link 3 is an elliptic follower. Links 2 and 3 are in contact with each other at H through a sliding contact. Points P and Q are the centers of the circle and of the ellipse, respectively.

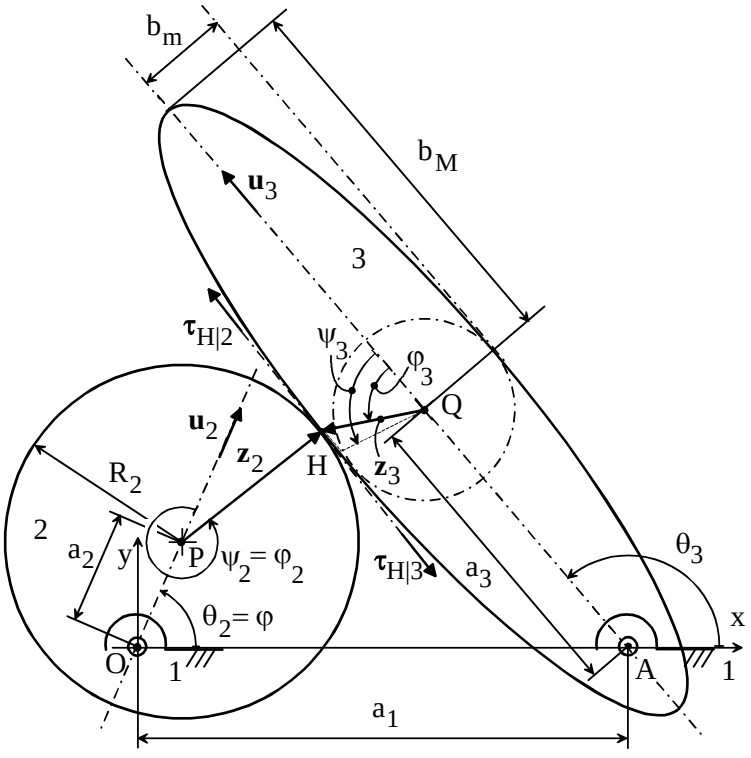

Figure 6: A circular cam with an elliptic follower: notation.

5.3.1. Position Analysis

With reference to Fig. 6, R_2, b_m and b_M are the radius of the circular cam, the semi-minor and the semi-major axes of the elliptic follower, respectively; whereas, a_1, a_2, and a_3 are the lengths of the segments OA, OP, and AQ, respectively. The angles ψ_2 and ψ_3 are the adopted curve parameters. Therefore, the parametric equations of the conjugate profiles and the analytic expressions of the unit complex number $\boldsymbol{\tau}_{H|2}$ and $\boldsymbol{\tau}_{H|3}$ are as follows:

- link 2 (circular cam): $h_2=R_2$ and $\varphi_2=\psi_2$, which yield $\mathbf{h}_2=h_2\exp(\mathbf{i}\varphi_2)\equiv x_{H|2}+\mathbf{i}y_{H|2}$, that is, $x_{H|2}=R_2\cos\psi_2$, $y_{H|2}=R_2\sin\psi_2$, and $\boldsymbol{\tau}_{H|2} = \mathbf{i}\exp(\mathbf{i}\,\psi_2)$;
- link 3 (elliptic follower): $\mathbf{h}_3=h_3\exp(\mathbf{i}\varphi_3)\equiv x_{H|3}+\mathbf{i}y_{H|3}$ with $x_{H|3}=b_M\cos\psi_3$, $y_{H|3}=b_m\sin\psi_3$ which yield

$$h_3=\sqrt{b_M^2\cos^2\psi_3+b_m^2\sin^2\psi_3}\,,\quad \varphi_3=\operatorname{atan2}(b_m\sin\psi_3,b_M\cos\psi_3),\quad \text{and}\quad \boldsymbol{\tau}_{H|3}=\frac{-b_M\sin\psi_3+\mathbf{i}b_m\cos\psi_3}{\sqrt{b_m^2\cos^2\psi_3+b_M^2\sin^2\psi_3}}$$

With the adopted notations, the following relationships hold:

$$\mathbf{z}_2 = R_2\exp(\mathbf{i}\psi_2)\,\mathbf{u}_2,\quad \mathbf{z}_3 = (b_M\cos\psi_3+\mathbf{i}\,b_m\sin\psi_3)\,\mathbf{u}_3, \tag{57a}$$

$$\mathbf{z}_P = a_2\,\mathbf{u}_2,\quad \mathbf{z}_Q = a_1 + a_3\,\mathbf{u}_3 \tag{57b}$$

where $\mathbf{u}_k=\exp(\mathbf{i}\theta_k)$ for k=2,3.

The introduction of expressions (57a) and (57b) into Eq. (3) yields, for the mechanism of Fig. 6, the following loop equation:

$$[a_2 + R_2\exp(\mathbf{i}\,\psi_2)]\,\mathbf{u}_2 = a_1 + [(a_3 + b_M\cos\psi_3) + \mathbf{i}\,b_m\sin\psi_3]\,\mathbf{u}_3 \tag{58}$$

Moreover, the introduction of the above-reported expressions for $\mathbf{h}_2$ and $\mathbf{h}_3$ into Eq. (6) gives the auxiliary constraint equation

$$(\cos\psi_2\sin\psi_3 - d\,\sin\psi_2\cos\psi_3)\cos(\theta_2-\theta_3) - (\sin\psi_2\sin\psi_3 + d\,\cos\psi_2\cos\psi_3)\sin(\theta_2-\theta_3) = 0 \tag{59}$$

where $d=b_m/b_M$.

Equations (58) and (59) constitute the complete set of constraint equations of this mechanism. They form a system of three scalar equations in four unknowns: θ_2, θ_3, ψ_2, and ψ_3. θ_2 is chosen as generalized coordinate φ of the mechanism; the remaining 3 variables are all secondary variable whose expression as a function of φ can be computed by solving the constraint equation system. The analytic solution of such system is not straightforward and can be numerically implemented. A simple geometric reasoning shows that, for a fixed position of the circular cam (i.e., for assigned θ_2), only two positions (i.e., two values of θ_3) of the elliptic follower make it touch the cam, that is, the PA has only two real solutions (i.e., there are only two assembly modes). Figure 7 shows the mechanism motion in the two possible assembly modes.

5.3.2. Velocity Analysis

The 1st time derivative of the constraint-equation system constituted by Eqs. (58) and (59) yields

$$\dot\theta_2\,D(\theta_2) = 0 \tag{60a}$$

$$\dot\theta_2\,L_{Sc}(\theta_2) = 0 \tag{60b}$$

where

$$D(\theta_2) = \mathbf{g}_1\,\nu_3 - \mathbf{g}_2\,\varepsilon_2 + \mathbf{g}_3\,\varepsilon_3 - \mathbf{g}_0 \tag{61a}$$

$$L_{Sc}(\theta_2) = (\nu_3 - \varepsilon_2 - 1)\,h_1 + \varepsilon_3\,h_2 \tag{61b}$$

with

$$\mathbf{g}_0 = \mathbf{i}\,[a_2 + R_2\exp(\mathbf{i}\,\psi_2)]\,\mathbf{u}_2,\quad \mathbf{g}_1 = \mathbf{i}\,[(a_3 + b_M\cos\psi_3) + \mathbf{i}\,b_m\sin\psi_3]\,\mathbf{u}_3,$$

$$\mathbf{g}_2 = \mathbf{i}\,R_2\exp(\mathbf{i}\,\psi_2)\,\mathbf{u}_2,\quad \mathbf{g}_3 = [-b_M\sin\psi_3 + \mathbf{i}\,b_m\cos\psi_3]\,\mathbf{u}_3,$$

$$h_1 = (\cos\psi_2\sin\psi_3 - d\,\sin\psi_2\cos\psi_3)\sin(\theta_2-\theta_3) + (\sin\psi_2\sin\psi_3 + d\,\cos\psi_2\cos\psi_3)\cos(\theta_2-\theta_3),$$

$$h_2 = (\cos\psi_2\cos\psi_3 + d\,\sin\psi_2\sin\psi_3)\cos(\theta_2-\theta_3) - (\sin\psi_2\cos\psi_3 - d\,\cos\psi_2\sin\psi_3)\sin(\theta_2-\theta_3),$$

and

$$\nu_3 = \frac{\dot\theta_3}{\dot\theta_2};\qquad \varepsilon_2 = \frac{\dot\psi_2}{\dot\theta_2};\qquad \varepsilon_3 = \frac{\dot\psi_3}{\dot\theta_2}.$$

Therefore, the VA equations obtained by equating to zero $D(\theta_2)$ and $L_{Sc}(\theta_2)$ (see Eqs.(27a) and (27c)) are

$$\mathbf{g}_1\,\nu_3 - \mathbf{g}_2\,\varepsilon_2 + \mathbf{g}_3\,\varepsilon_3 = \mathbf{g}_0 \tag{62a}$$

$$h_1\,\nu_3 - h_1\,\varepsilon_2 + h_2\,\varepsilon_3 = h_1 \tag{62b}$$

where all the coefficients, $\mathbf{g}_i$ for i=0,1,2,3 and h_j for j=1,2, are known after the solution of the PA.

The solution of system (62) is:

$$\varepsilon_2 = \frac{\mathrm{Im}\left\{(\mathbf{g}_0 - \mathbf{g}_1)\underline{\left[\mathbf{g}_3 - \left(h_2/h_1\right)\mathbf{g}_1\right]}\right\}}{\mathrm{Im}\left\{(\mathbf{g}_1 - \mathbf{g}_2)\underline{\left[\mathbf{g}_3 - \left(h_2/h_1\right)\mathbf{g}_1\right]}\right\}}, \quad \varepsilon_3 = \frac{\mathrm{Im}\left\{(\mathbf{g}_0 - \mathbf{g}_1)\underline{(\mathbf{g}_1 - \mathbf{g}_2)}\right\}}{\mathrm{Im}\left\{\underline{\left[\mathbf{g}_3 - \left(h_2/h_1\right)\mathbf{g}_1\right]}\underline{(\mathbf{g}_1 - \mathbf{g}_2)}\right\}}, \tag{63a}$$

$$\nu_3 = 1 + \varepsilon_2 - (h_2/h_1)\,\varepsilon_3 \tag{63b}$$

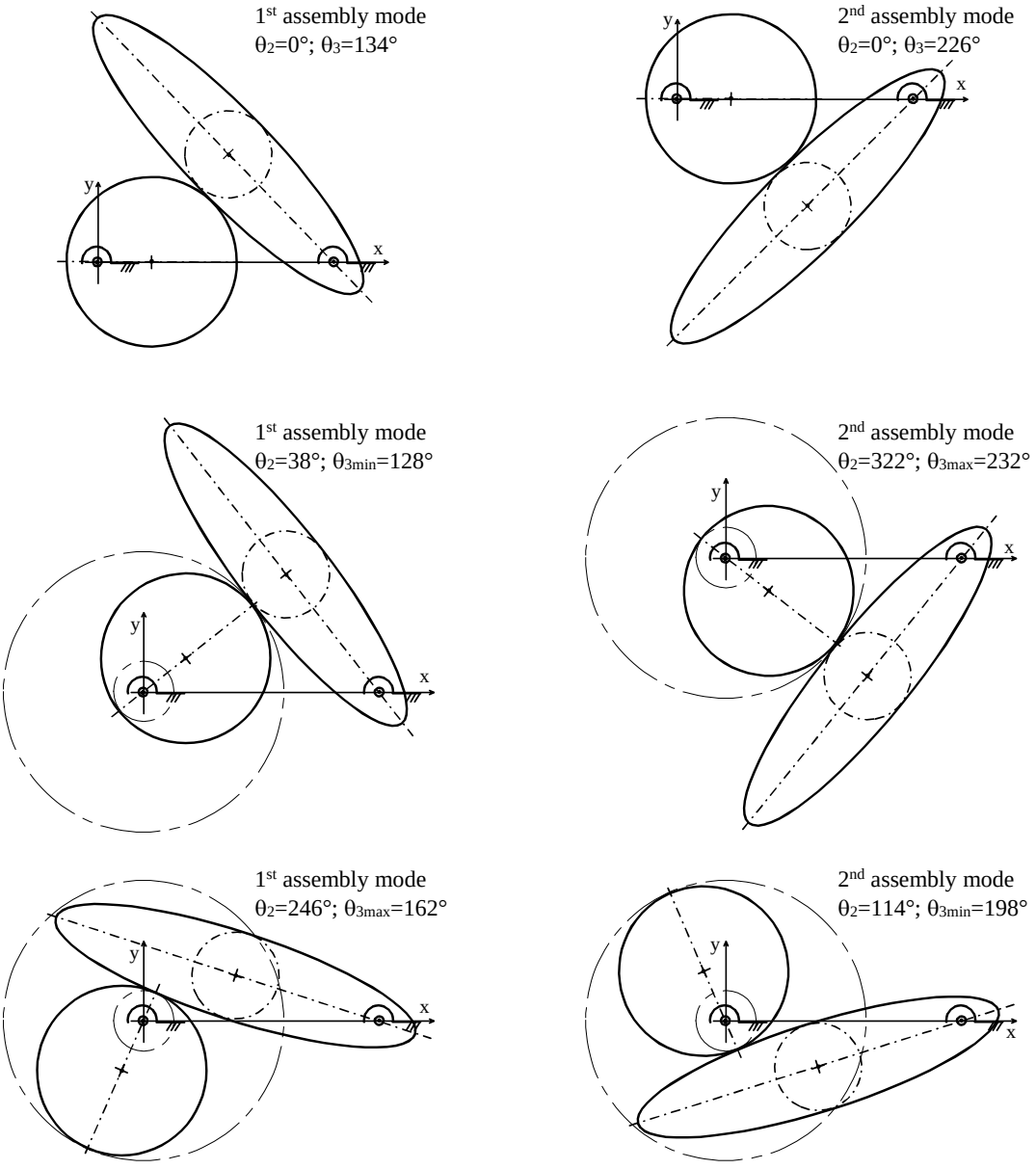

Figure 7: Motion simulation of a circular cam with an elliptic follower: the initial configuration (θ_2=0°) and the two extreme positions of the follower for the two PA solutions (assembly modes) in the case (R_2/a_1)=0.362, (a_2/a_1)=0.231, (a_3/a_1)=0.635, (b_M/a_1)=0.807, and (b_m/a_1)=0.188.

5.2.3. Acceleration Analysis

The time derivative of system (60) provides the following equations (see Eqs. (29a) and (29c))

$$\ddot{\theta}_2\, D(\theta_2) + \dot{\theta}_2^2[E(\theta_2) - F(\theta_2)] = 0 \tag{64a}$$

$$\ddot{\theta}_2\, L_{Sc}(\theta_2) + \dot{\theta}_2^2[M_{Sc}(\theta_2) + G_{Sc}(\theta_2)] = 0 \tag{64b}$$

where

$$E(\theta_2) = \mathbf{g}_1 \lambda_3 - \mathbf{g}_2 \eta_2 + \mathbf{g}_3 \eta_3 \tag{65a}$$

$$F(\theta_2) = [a_3 \nu_3^2 + (b_M \cos\psi_3 + \mathbf{i}\, b_m \sin\psi_3)(\nu_3^2 + \varepsilon_3^2) + 2(b_m \cos\psi_3 + \mathbf{i}\, b_M \sin\psi_3)\nu_3 \varepsilon_3]\,\mathbf{u}_3 + - [R_2 \exp(\mathbf{i}\,\psi_2)(1+\varepsilon_2)^2 + a_2]\,\mathbf{u}_2 \tag{65b}$$

$$M_{Sc}(\theta_2) = \lambda_3 h_1 - \eta_2 h_1 + \eta_3 h_2, \qquad G_{Sc}(\theta_2) = 2(\nu_3 - \varepsilon_2 - 1)\varepsilon_3 p_1 - [(\nu_3 - \varepsilon_2 - 1)^2 + \varepsilon_3^2] p_2 \tag{65c}$$

with

$$p_1 = (\cos\psi_2 \cos\psi_3 + d \sin\psi_2 \sin\psi_3)\sin(\theta_2 - \theta_3) + (\sin\psi_2 \cos\psi_3 - d \cos\psi_2 \sin\psi_3)\cos(\theta_2 - \theta_3)$$

$$p_2 = (\cos\psi_2 \sin\psi_3 - d \sin\psi_2 \cos\psi_3)\cos(\theta_2 - \theta_3) - (\sin\psi_2 \sin\psi_3 + d \cos\psi_2 \cos\psi_3)\sin(\theta_2 - \theta_3)$$

and

$$\lambda_3 = \frac{d\nu_3}{d\theta_2}; \qquad \eta_2 = \frac{d\varepsilon_2}{d\theta_2}; \qquad \eta_3 = \frac{d\varepsilon_3}{d\theta_2}.$$

Therefore, in this case, the AA equations (see Eqs.(31a) and (31c)) are

$$\mathbf{g}_1 \lambda_3 - \mathbf{g}_2 \eta_2 + \mathbf{g}_3 \eta_3 = F(\theta_2) \tag{66a}$$

$$\lambda_3 h_1 - \eta_2 h_1 + \eta_3 h_2 = -G_{Sc}(\theta_2) \tag{66b}$$

where $F(\theta_2)$ and $G_{Sc}(\theta_2)$ (see Eqs. (65)) are known after the solution of the PA and of the VA.

The solution of system (66) is:

$$\eta_2 = \frac{\mathrm{Im}\left\{\left[F(\theta_2) + \mathbf{g}_1 G_{Sc}(\theta_2)/h_1\right]\underline{\left[\mathbf{g}_3 - (h_2/h_1)\mathbf{g}_1\right]}\right\}}{\mathrm{Im}\left\{(\mathbf{g}_1 - \mathbf{g}_2)\underline{\left[\mathbf{g}_3 - (h_2/h_1)\mathbf{g}_1\right]}\right\}}, \quad \eta_3 = \frac{\mathrm{Im}\left\{\left[F(\theta_2) + \mathbf{g}_1 G_{Sc}(\theta_2)/h_1\right]\underline{(\mathbf{g}_1 - \mathbf{g}_2)}\right\}}{\mathrm{Im}\left\{\left[\mathbf{g}_3 - (h_2/h_1)\mathbf{g}_1\right]\underline{(\mathbf{g}_1 - \mathbf{g}_2)}\right\}} \tag{67a}$$

$$\lambda_3 = \eta_2 - (h_2/h_1)\eta_3 - G_{Sc}(\theta_2)/h_1 \tag{67b}$$

6. Conclusions

The auxiliary equations, necessary to model higher pairs in planar mechanisms, have been reformulated in the frame of the complex-number method. This reformulation makes the complex-number method able to write the complete set of constraint equations of planar mechanisms.

The so-extended complex-number method has been used to build a general notation for writing the constraint equations of planar mechanisms. The proposed notation can be adopted for developing a general purpose software that writes and solves the constraint-equation system of any planar mechanism, and could be the kinematic block of a multi-body simulation environment devoted to planar mechanisms.

The presented notation has been used to propose a general algorithm for solving the kinematic-analysis problems of single-DOF planar mechanisms. Such algorithm is based on the systematic use of the velocity coefficients (VCs) and of the acceleration coefficients (ACs). It introduces one VC and one AC for each mobile link, and determines them by sequentially solving two linear systems with the same coefficient matrix of the unknowns; then, it computes any velocity/acceleration of the mechanism by using the so-computed VCs and ACs. The proposed algorithm is globally new and simple enough to present planar kinematics in graduate and/or undergraduate courses.

The effectiveness of the proposed algorithm has been proved by applying it to three relevant single-DOF planar mechanism: the shaper mechanism, a kinematic inversion of the geared five-bar mechanism, and a circular cam with an elliptic follower.

Acknowledgments

This work has been developed at the Laboratory of Mechatronics and Virtual Prototyping (LaMaViP) of Ferrara Technopole, supported by FAR2017 UNIFE funds.

References

1. Paul, B.: Kinematics and Dynamics of Planar Machinary. Prentice-Hall, Inc., Englewood Cliffs N.J. (1987).
2. Nikravesh, P.E.: Planar Multibody Dynamics. CRC Press, Boca Raton FL (2018).
3. Marghitu, D.B.: Mechanisms and Robots Analysis with MATLAB. Springer-Verlag, London, (2009).
4. Galletti, C.U.: A Note on Modular Approaches to Planar Linkage Kinematic Analysis. Mech. Mach. Theory 21(5), 385-391 (1986).
5. Bràt, V., Lederer, P.: KIDYAN: Computer-Aided Kinematic and Dynamic Analysis of Planar Mechanisms. Mech. Mach. Theory 8, 457-467 (1973).
6. Wampler, C.: Solving the Kinematics of Planar Mechanisms. J. Mech. Des 121(3), 387-391 (1999).

7. Wampler, C.: Solving the Kinematics of Planar Mechanisms by Dixon Determinant and a Complex-Plane Formulation. J. Mech. Des 123(3), 382-387 (2001).
8. IFToMM Commission A: Terminology for the Theory of Machines and Mechanisms. Mech. Mach. Theory 26(5), 435-539 (1991).
9. Barton, L.O.: Mechanism Analysis, Simplified and Graphical Techniques, 2nd Ed. CRC Press, Boca Raton FL (1993).
10. Uicker, J.J., Pennock, G. R., Shigley, J.E.: Theory of Machines and Mechanisms, 3rd Ed. Oxford University Press, Oxford UK (2003).
11. Haug, E.J.: Computer Aided Kinematics and Dynamics of Mechanical Systems. Allyn and Bacon, Needham Heights MA (1989).
12. Di Gregorio, R.: An Algorithm for Analytically Calculating the Positions of the Secondary Instant Centers of Indeterminate Linkages. J. Mech. Des 130(4), 042303-(1-9) (2008)
13. Di Gregorio, R.: A novel dynamic model for single-degree-of-freedom planar mechanisms based on instant centers. ASME J. of Mechanisms and Robotics 8(1), 011013-(8pages) (2016).
14. Di Gregorio, R.: On the Use of Instant Centers to Build Dynamic Models of Single-dof Planar Mechanisms. In: Lenarcic J., Parenti-Castelli V. (eds) Advances in Robot Kinematics 2018. Springer Proceedings in Advanced Robotics, vol 8, pp. 242-249. Springer, Cham (2018)
15. Rothbart, H.A.: Cam Design Handbook. McGraw-Hill,Inc., New York NY (2004).
16. Norton, R.L., Cam Design and Manufacturing Handbook, 2nd Ed. Industrial Press, New York NY (2009).
17. Litvin, F.L., Fuentes-Aznar, A., Gonzalez-Perez, I., Hayasaka, K.: Noncircular Gears: Design and Generation. Cambridge University Press, Cambridge UK (2009).
18. Freudenstein, F., Primerose, E.J.F.: Geared Five-Bar Motion: Part 1 – Gear Ratio Minus One. ASME J. of Applied Mechanics 30(2), 161-169 (1963).
19. Primerose, E.J.F., Freudenstein, F.: Geared Five-Bar Motion: Part 2 – Arbitrary Commensurate Gear Ratio. ASME J. of Applied Mechanics 30(2), 170-175 (1963).
20. Zhao, J., Feng Z., Ma N., Chu F.: Kinematic Design of Geared Five-Bar Linkage. In: Zhao J. et al. Design of Special Planar Linkages, pp.51-75, Springer, Heidelberg (2014).
21. Sandhya, R, Kadam, M., Balamurugan, G., Rangavittal, H.K.: Synthesis and Analysis of Geared Five Bar Mechanism for Ornithopter Applications. In: Procs. of 2nd International and 17th National Conference on Machines and Mechanisms, pp. iNaCoMM2015-218 (10 pages), IIT Kanpur, Kanpur IN (2015).
22. Kleiner, I.: Thinking the Unthinkable: the Story of Complex Numbers (with a Moral). Mathematics Teacher 81, 583-592 (Oct., 1988).
23. Zwikker, C.: The Advanced Geometry of Plane Curves and Their Applications. Dover Publications, Inc., New York USA (1963, reprint of “Advanced Plane Geometry” published in 1950).
24. Luck, K., Modler, K.-H.: Getriebetechnik. Analyse, Synthese und Optimierung. 2nd Ed. Springer-Verlag, Berlin DE (1995).
25. Dijksman, E. A.: Motion Geometry of Mechanisms. Cambridge University Press, Cambridge UK (1976)

Figure Captions

Figure 1: A conjugate profile fixed to the k-th link of a planar mechanism: notation.

Figure 2: Two conjugate profiles in contact with each other at point H.

Figure 3: Notations: k-th link, traversed by q ICs, in contact with the w-th link at A_{p+i} through an higher pair, and containing the linear guide of a P-pair that connects it to a slider fixed in the s-th link.

Figure 4: Shaper mechanism: kinematic scheme (link 1 is the frame) and notations (A_1xy is the reference of an Argand plane where $\mathbf{z}=x+\mathbf{i}y$).

Figure 5: Kinematic scheme of a kinematic inversion of the geared five-bar mechanism [a rolling contact occurs at point H; the planet carrier (link 5) hinged at P and Q to the gears 2 and 3, respectively, is not shown since it does not affect the mechanism motion].

Figure 6: A circular cam with an elliptic follower: notation.

Figure 7: Motion simulation of a circular cam with an elliptic follower: the initial configuration ($\theta_2=0°$) and the two extreme positions of the follower for the two PA solutions (assembly modes) in the case $(R_2/a_1)=0.362$, $(a_2/a_1)=0.231$, $(a_3/a_1)=0.635$, $(b_M/a_1)=0.807$, and $(b_m/a_1)=0.188$.

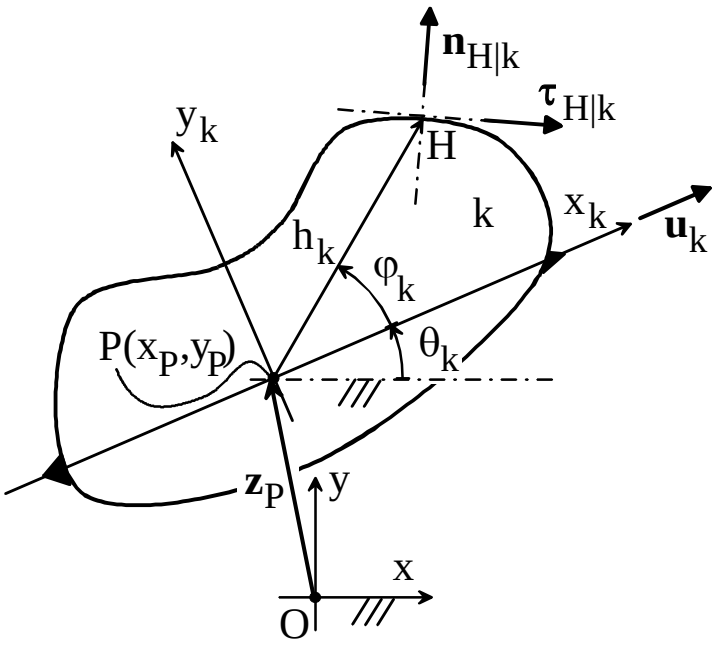

Figure 1: A conjugate profile fixed to the k-th link of a planar mechanism: notation.

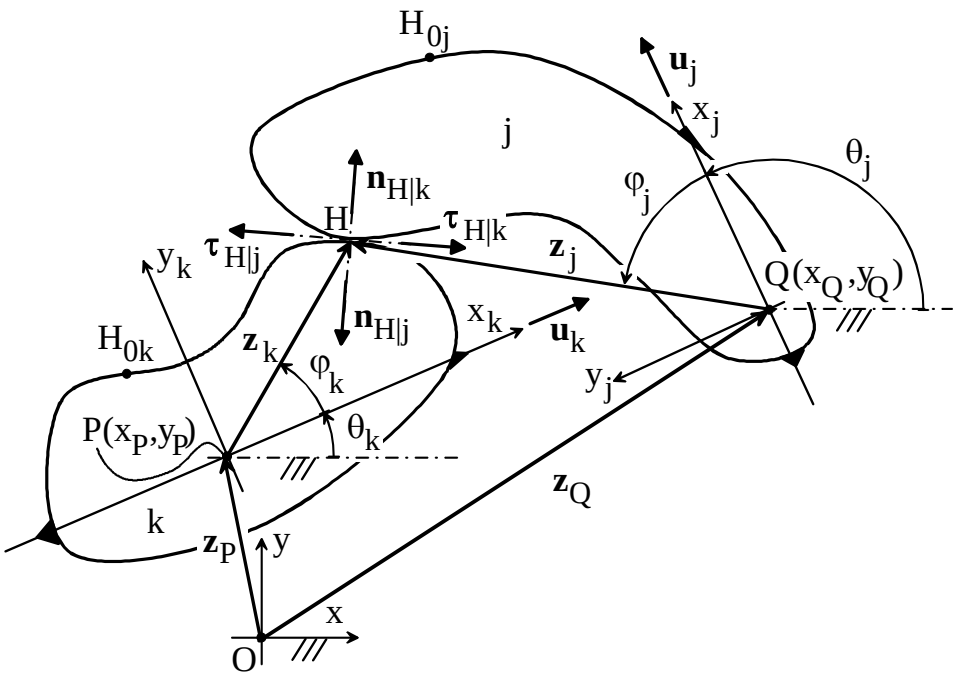

Figure 2: Two conjugate profiles in contact with each other at point H.

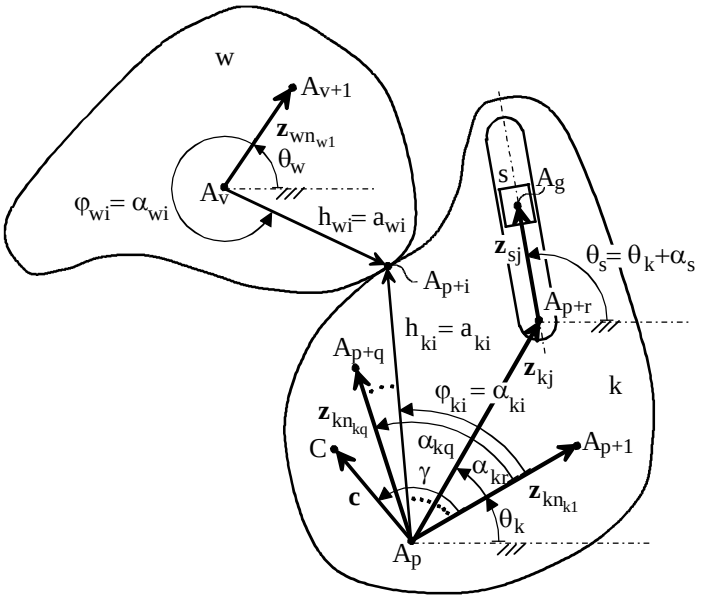

Figure 3: Notations: k-th link, traversed by q ICs, in contact with the w-th link at A_{p+i} through an higher pair, and containing the linear guide of a P-pair that connects it to a slider fixed in the s-th link.

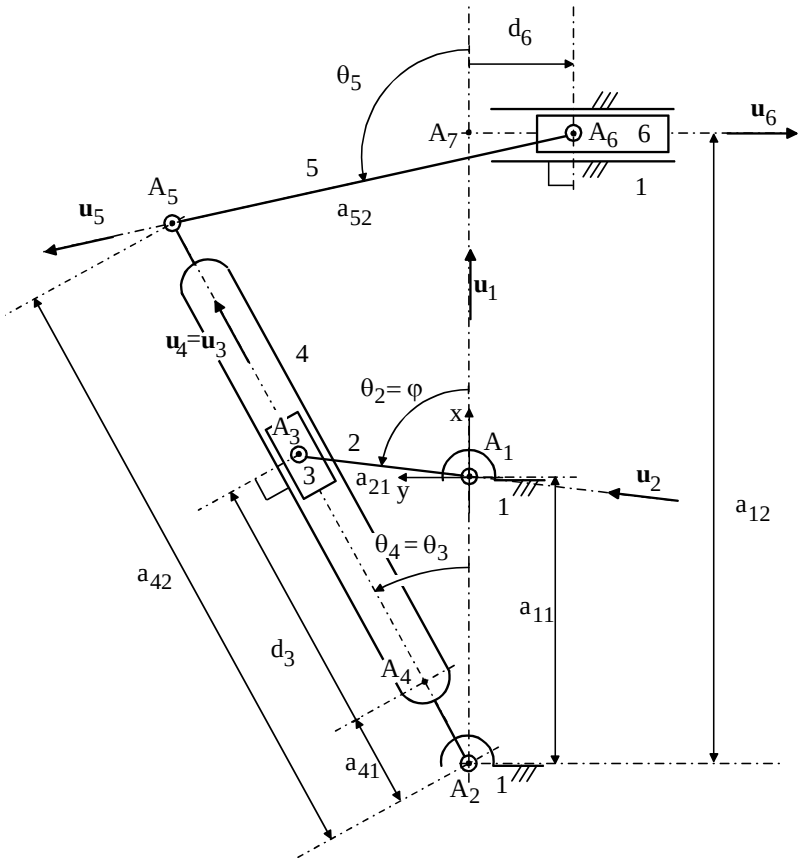

Figure 4: Shaper mechanism: kinematic scheme (link 1 is the frame) and notations (A_1xy is the reference of an Argand plane where **z**=x+**i**y).

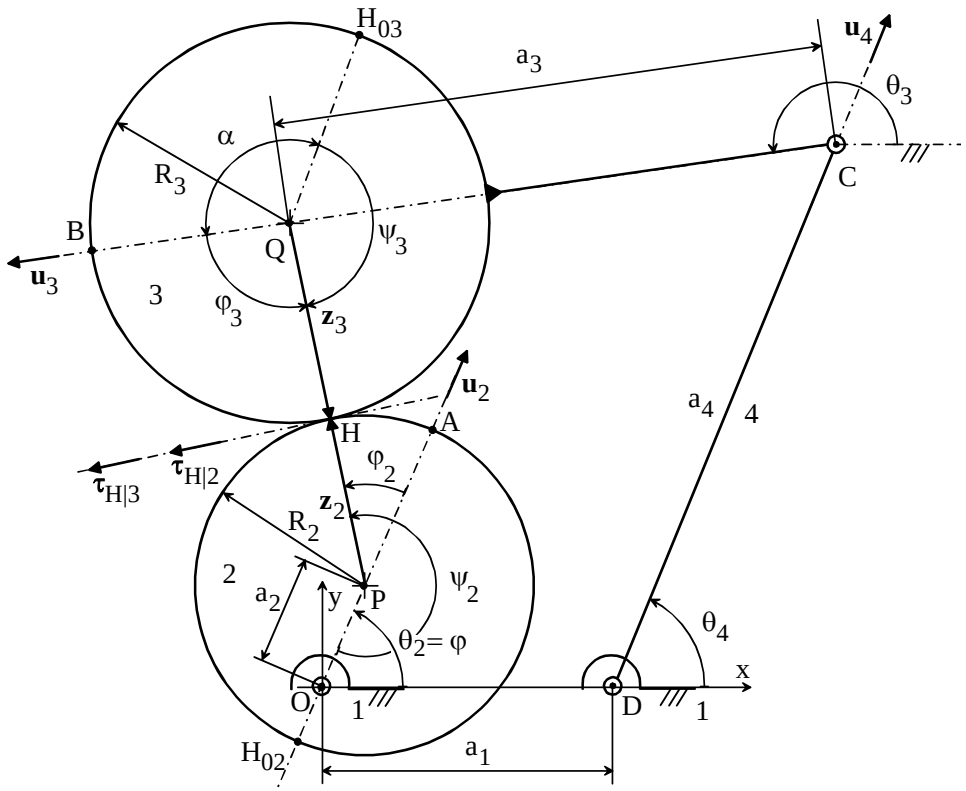

Figure 5: Kinematic scheme of a kinematic inversion of the geared five-bar mechanism [a rolling contact occurs at point H; the planet carrier (link 5) hinged at P and Q to the gears 2 and 3, respectively, is not shown since it does not affect the mechanism motion].

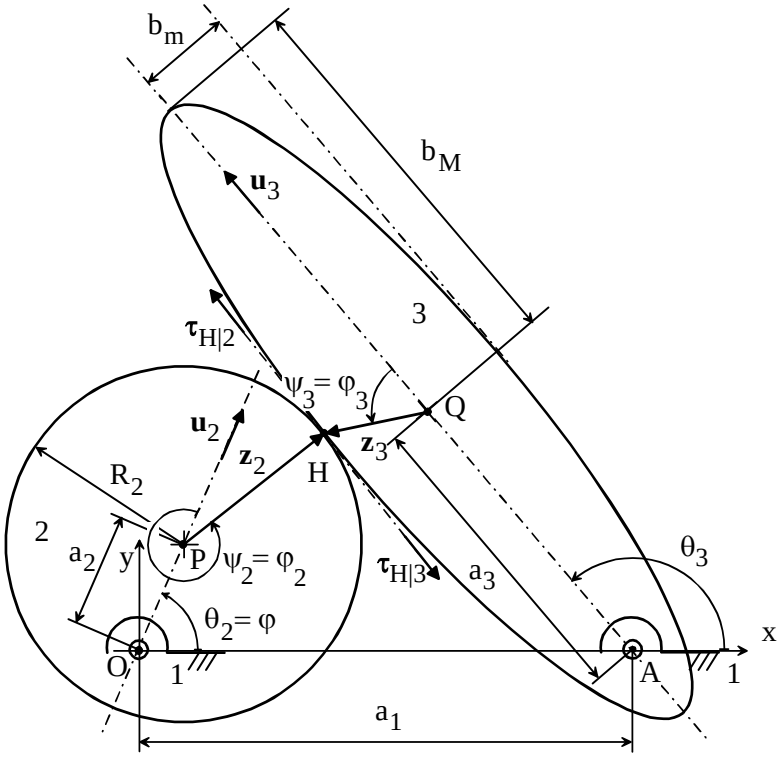

Figure 6: A circular cam with an elliptic follower: notation.

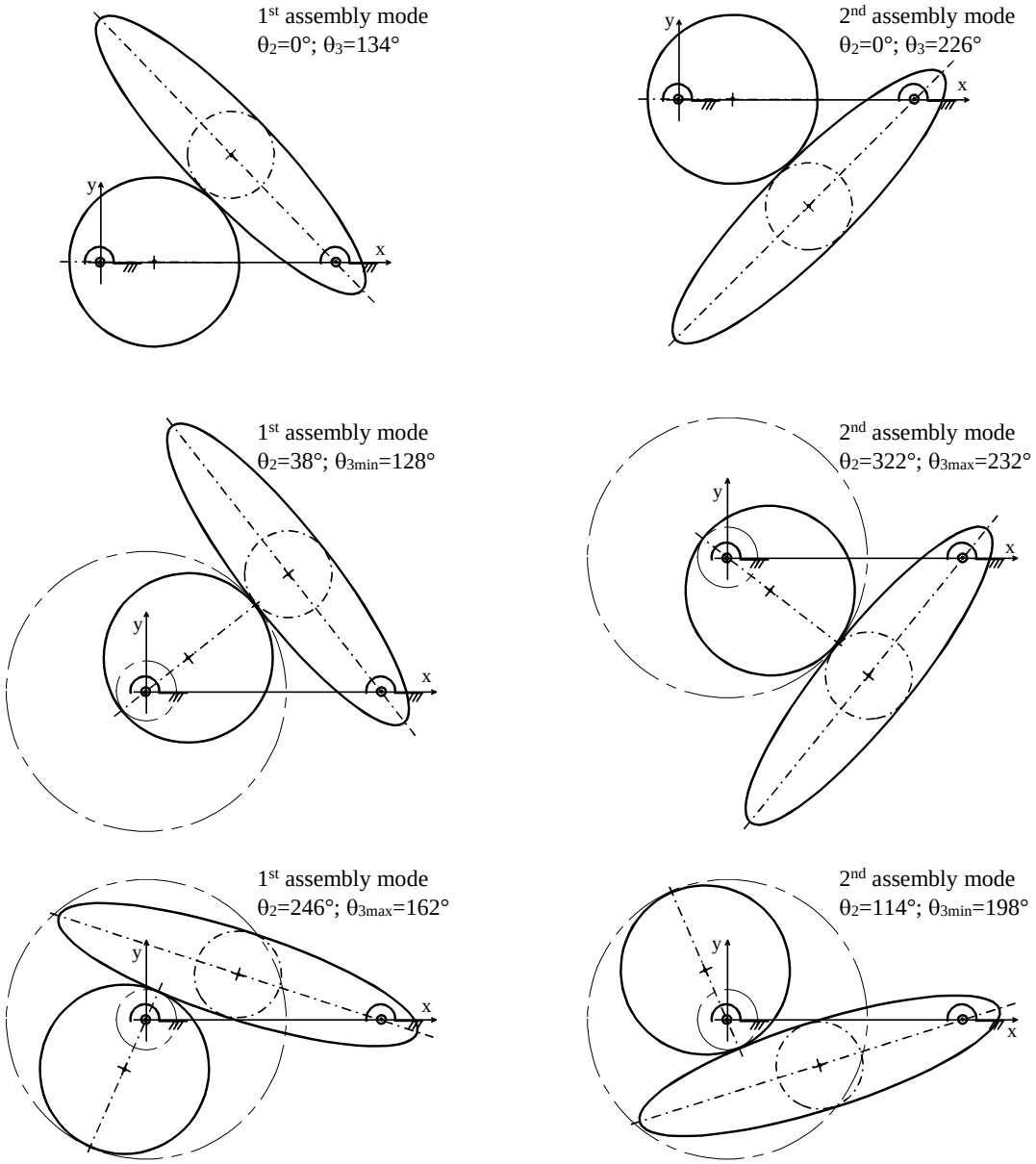

Figure 7: Motion simulation of a circular cam with an elliptic follower: the initial configuration (θ_2=0°) and the two extreme positions of the follower for the two PA solutions (assembly modes) in the case (R_2/a_1)=0.362, (a_2/a_1)=0.231, (a_3/a_1)=0.635, (b_M/a_1)=0.807, and (b_m/a_1)=0.188.